Ann. Rev. Earth Planet. Sci. 1981. 9:345–83

INTERVALENCE TRANSITIONS IN MIXED-VALENCE MINERALS OF IRON AND TITANIUM

Roger G. Burns
Department of Earth and Planetary Sciences, Massachusetts Institute of Technology, Cambridge, Massachusetts 02139

> Since ferrous iron usually colors minerals green, and ferric iron yellow or brown, it may seem rather remarkable that the presence of both together should give rise to a blue color, as in the case of vivianite. . . . . Other instances may perhaps be discovered, should this subject ever be investigated as it deserves to be.
>
> E. T. Wherry, *Am. Mineral.* 3:161 (1918)

> This term (charge transfer) is used as a catch phrase for a wide variety of electronic processes which give rise to strong absorption in the visible and ultraviolet and there is a great danger in merely assigning any unexplained feature in a spectrum as a "charge transfer band."
>
> W. B. White, *Am. Mineral.* 52:555 (1967)

INTRODUCTION

Mixed-valence minerals containing an element in two different oxidation states frequently have unusual physical properties, one of which is intense coloration originating from the transfer of electrons between the two valence states. Interpretations of such "charge transfer" or intervalence transitions in absorption spectra of minerals have often been controversial. The two statements cited in the preface above convey the anticipation, excitement, and frustrations of research on mixed-valence transition metal-bearing minerals, which have been compounded during the past decade as a result of spectral measurements on extraterrestrial materials from the Moon and meteorites.

0084-6597/81/0515-0345$01.00

Nevertheless, light-induced electron transfer processes between neighboring elements in a crystal structure continue to have important applications in the earth and planetary sciences. Not only do they affect color and pleochroism, visible-region and nuclear gamma resonance (Mössbauer) spectra, magnetism, electrical and thermal conductivities of minerals, but they also manifest themselves in such wide-ranging phenomena as geophysical properties of the Earth's interior, remote-sensed spectra of planetary surfaces, and transition metal geochemistry. Recent investigations of mixed-valence compounds (Brown 1980) have greatly clarified electron transfer processes in minerals (Burns et al 1980). This review focusses on results and applications of such measurements for silicates and oxides of iron and titanium, the most abundant transition elements.

Mixed-valence minerals have attracted attention since antiquity. The subtle blue hues of the gems sapphire, aquamarine, and iolite, the intense colorations of certain amphiboles, micas, tourmalines, and pyroxenes, and the opacity of magnetite, ilmenite, etc, were generally attributed to the transfer of electrons between Fe^{2+} and Fe^{3+} ions (Watson 1918, MacCarthy 1926, Weyl 1951, Martinet & Martinet 1952). The highly directional character of such "charge transfer" interactions in minerals was demonstrated by absorption spectral measurements in polarized light (Faye et al 1968) and electrical conductivity measurements (Littler & Williams 1965). While the spectral features due to $Fe^{2+} \rightarrow Fe^{3+}$ charge transfer transitions could usually be distinguished from crystal field transitions within individual Fe^{2+} and Fe^{3+} ions, complexities arose when titanium was present. The color and spectra of blue kyanites and sapphire, for example, have sparked considerable debate (White & White 1967, Faye & Nickel 1969a, Lehmann & Harder 1970, Faye 1971, Smith 1978b). Subsequently, the occurrence of Ti^{3+} ions in natural and synthetic pyroxenes and glasses in terrestrial and extraterrestrial rocks led to further problems of distiguishing Ti^{3+} crystal field transitions from $Ti^{3+} \rightarrow Ti^{4+}$ and $Fe^{2+} \rightarrow Ti^{4+}$ charge transfer transitions (Dowty & Clark 1973a,b, Burns & Huggins 1973, Mao & Bell 1974). Some of these opposing spectral assignments of Fe-Ti-bearing silicates and oxide minerals are addressed in this review.

Another area of interest in mixed-valence minerals concerns the nature and extent of electron transfer processes in the crystal structures. Here the question is whether electron hopping is localized on adjacent cations leading to discrete valencies (e.g. distinguishable Fe^{2+} and Fe^{3+} ions), or whether electrons are delocalized along chains of cations leading to indistinguishable valencies. These phenomena are affected not only by crystal chemical and structural factors, but also by variations of pressure

and temperature. This review highlights pertinent crystal structure data for mixed-valence minerals of iron and titanium and temperature-pressure variations of their electronic absorption and Mössbauer spectra.

TERMINOLOGY

In mixed-valence minerals, we are primarily interested in the excitation of electrons *between* adjacent ions and not within individual cations. The latter intra-electronic or crystal field transitions take place between d or f orbital energy levels of single transition metal ions. Electronic transitions between neighboring ions are broadly called charge transfer (CT) transitions and include anion → cation as well as cation → cation transitions. In oxides and silicates, oxygen → cation CT transitions are generally excited by higher energy ultraviolet radiation, but absorption edges may extend into the visible region and induce dark brown colors in a mineral (e.g. biotite, hornblende). For cations most frequently encountered in terrestrial and lunar minerals, oxygen → cation CT energies for octahedrally coordinated cations are calculated or observed to decrease in the order (Loeffler et al 1974)

$$Cr^{3+} > Ti^{3+} > Fe^{2+} > Ti^{4+} > Fe^{3+}.$$

The focus of this review, however, is on electron transfer between adjacent cations which momentarily change valence during the lifetime of the transition. Such electron exchange processes are referred to as intervalence transitions. The cation → cation intervalence transitions are classified as either homonuclear (e.g. $Fe^{2+} \rightarrow Fe^{3+}$; $Ti^{3+} \rightarrow Ti^{4+}$) or heteronuclear (e.g. $Fe^{2+} \rightarrow Ti^{4+}$), and are typically induced by incident light in the visible–short wave infrared region (wavelengths 400–2000 nm or wave numbers 25,000–4,000 cm^{-1}). Light-induced intervalence transitions are sometimes referred to as optically excited electron exchange transitions, energies of which are denoted by E_{OP}.

In order for intervalence transitions to occur the interacting cations must be adjacent to one another in the mineral crystal structure. Therefore, they are generally observed between transition metal ions in coordination sites sharing edges or faces. The majority of $Fe^{2+} \rightarrow Fe^{3+}$ and $Fe^{2+} \rightarrow Ti^{4+}$ CT transitions identified in silicate and oxide minerals involve cations in edge-shared octahedra, although examples involving face-shared octahedra (sapphire), edge-shared octahedra-tetrahedra (cordierite) and edge-shared cube-tetrahedra (garnet) are known.

A classification scheme for mixed valence compounds has been developed (Robin & Day 1967, Day 1976) based on the degree to which the sites

occupied by the cations of differing valence can be distinguished in the ground state and the consequent ease or difficulty of transferring an electron from one site to another. When the two sites are very different (e.g. Fe^{3+}-bearing octahedral and Fe^{2+}-bearing cube sites in the garnet structure), the transfer of electrons is difficult so that the properties of the mineral are essentially the sum of those of the individual cations in the two sites. These are termed Class I compounds (Day 1976). If the two sites are identical, the electron can be transferred from one site to the other with no expenditure of energy. If the structure contains continuous arrays of sites, the mineral will have metallic properties. Because the valencies of the individual ions are "smeared out" the characteristic properties of the single valence states may not be found. Materials of this kind are called Class IIIB compounds. Magnetite is the classic example of a Class IIIB compound. If the structure is not completely continuous, electron delocalization only takes place within a finite cluster of equivalent cations. Although the individual ion properties may not be seen the structure does not conduct electrons. This type of substance is called a Class IIIA compound.

Intermediate between these two extremes are minerals classified as Class II compounds in which the two sites are similar but distinguishable (i.e. both are octahedral sites, but with slightly different metal-oxygen distances, or ligand orientation or bond-type, such as the mica M1 and M2 sites). Such materials still exhibit ions with discrete valencies, but have low energy intervalence CT bands and are semiconductors. The physical properties of each class of mixed-valence compound are summarized in Table 1.

This approach to mixed-valence compounds represents an essentially static model and takes no account of the dynamical behavior of either the nucleus or the electrons. Class III compounds will be observed, for example, only if electrons are transferred from cation to cation more rapidly than the ligand atoms constituting the coordination site can relax to equilibrium positions corresponding to the individual discrete valencies. Fe^{2+} ions, for example, require a larger site than Fe^{3+} ions, but there may be insufficient time for the coordination polyhedra to expand each time an electron is momentarily transferred from Fe^{3+} to Fe^{2+}. The frequencies of such lattice relaxation effects are temperature dependent, but at elevated temperatures electrons may overcome activation energies to transfer from cations of discrete valencies to become electron-delocalized species. The energy required for the adiabatic delocalization of an electron between two sites is denoted E_{AD}, and an approximate relationship between this thermal activated electron energy and the optically excited electron exchange energy, E_{OP} is (Hush 1967): $E_{AD} = E_{OP}/4$.

Table 1 Physical properties of classes of mixed-valence compounds (after Day, 1976).

Property	Class I	Class II	Class III A	Class III B
Nature of sites in crystal structure	Vastly different, e.g. cube-octahedron, octahedron-tetrahedron	Similar, e.g. octahedra with slightly different bond lengths or ligands	Identical, finite clusters, e.g. edge-shared octahedral dimers	Identical, continuous chains, e.g. chains of edge-shared octahedra
Optical absorption spectroscopy	No intervalence transitions in visible region	One mixed-valence transition in visible region; absorption bands intensify at elevated pressures and low temperatures	One or more mixed-valence transition in visible region; temperature lowers intensity of absorption bands, pressure intensifies	Opaque; metallic reflectivity in visible region
Electrical conductivity	Insulator; resistivity $> 10^{12}$ ohm cm	Semiconductor; resistivity $10–10^{8}$ ohm cm	Insulator or high resistance semiconductor	Metallic conductor; resistivity $10^{-2}–10^{-6}$ ohm cm
Magnetic properties	Diamagnetic or paramagnetic to very low temperature	Magnetically dilute; either ferro- or anti-ferromagnetic at low temperatures	Magnetically dilute	Pauli paramagnetism or ferro-magnetic with high Curie temperature
Mössbauer spectra	Spectra of constituent Fe ions; discrete Fe^{2+} and Fe^{3+} ions	Spectra of constituent Fe ions; discrete Fe^{2+} and Fe^{3+} ions	Electron-delocalized species contribute to spectra; higher contributions at elevated temperatures and pressures	Electron delocalized species contribute to spectra; higher contributions at elevated temperatures and pressures

One consequence of thermally activated electron delocalization behavior is that techniques such as Mössbauer spectroscopy, which might be expected to distinguish discrete Fe^{2+} and Fe^{3+} valencies from electron delocalized Fe cation species, will detect Class III compound behavior only if electrons are transferred between Fe^{2+} and Fe^{3+} ions in neighboring sites more rapidly than the lifetime of the Mössbauer transition (10^{-7} s) between the 14.41 keV ground and excited nuclear energy levels of ^{57}Fe. Thus, Mössbauer spectrum profiles of Class III compounds are expected to show significant temperature variations.

CRYSTAL STRUCTURE FEATURES

It is apparent that the classification and properties of mixed-valence compounds depend greatly on the nature and extent of coordination sites containing adjacent cations (Loeffler et al 1975, Burns et al 1980). Many of the electronic properties can be correlated with crystal structure features, including metal-oxygen (M-O) bond strength as evidenced by M-O distances; metal-oxygen-metal overlap indicated by metal-metal (M-M) distances; symmetries of coordination polyhedra, e.g. regular or distorted octahedra, tetrahedra, cubes; types of polyhedral linkages, e.g. face-shared, edge-shared, corner-shared; and orientation and extent of linked polyhedra, e.g. isolated pairs, chains, bands, sheets. Such structural features of mixed-valence oxide and silicate minerals of Fe and Ti are summarized in Table 2. Note that cation → cation intervalence transitions generally produce intense absorption bands in visible-region spectra only when light is polarized along the metal-metal directions in the crystal structures.

MINERALS WITH FE^{2+}-FE^{3+} OCTAHEDRAL CLUSTERS

Vivianite

Perhaps the best-known mixed-valence compound exhibiting a $Fe^{2+} \rightarrow Fe^{3+}$ intervalence transition is vivianite, $Fe_3(PO_4)_2.8H_2O$. Although the formula of this mineral is not indicative of a mixed-valence compound, freshly cleaved vivianite crystals or newly precipitated ferrous phosphate which are pale green turn blue when exposed to air. Such intense blue colorations are atypical of pure Fe(II) or Fe(III) compounds containing Fe^{2+} or Fe^{3+} ions octahedrally coordinated to oxygen ligands, and are indicative of an intervalence transition (Allen & Hush 1967, Hush 1967, Robin & Day 1967).

Table 2 Structural data for mixed-valence minerals of Fe and Ti

Mineral (formula)	Sites (coord. no.)	M-M distances (Å)	Polyhedral linkages (type of sharing; extent of M-M cluster)	References
vivianite $Fe_3(PO_4)_2.8H_2O$	Fe_A (6) Fe_B (6)	Fe_B-Fe_B = 2.85	edge: isolated clusters	Mori & Ito 1950
sapphire Al_2O_3/Fe,Ti	A1 (6)	$\perp c$ = 2.79 $\parallel c$ = 2.65	edge: finite clusters; face: isolated clusters	Newnham & de Haan 1962
kyanite Al_2SiO_5/Fe,Ti	Al_1 (6) Al_2 (6) Al_3 (6) Al_4 (6)	2.75–2.78	edge: infinite Al_1-Al_2; chains: isolated Al_1-Al_2, Al_2-Al_3, Al_1-Al_4, Al_2-Al_4 clusters; substitutional blocking by Al^{3+}	Burnham 1963
aquamarine (beryl) $Be_3Al_2Si_6O_{18}$	Al (6)	$\parallel c$ = 4.60	isolated octahedra; cations possibly in channels	Gibbs et al 1968
cordierite (iolite) $Al_3(Mg,Fe^{2+})_2(Al,Fe^{3+})Si_5O_{18}$	M (6) T_1 (4)	M-T_1 = 2.74	edge: isolated octahedral-tetrahedral clusters; cations possibly in channels	Gibbs 1966
osumilute $K(Mg,Fe^{2+})_2(Al,Fe^{3+})_3(Si,Al)_{12}O_{30}$	similar to cordierite	comparable to cordierite	similar to cordierite	Brown & Gibbs 1969
tourmaline $Na(Mg,Fe,Mn,Li,Al)_3(Al,Fe)_6(Si_6O_{18})(BO_3)_3(OH,F)_4$	Mg (6) Al (6)	Mg-Mg = 3.04 Mg-Al = 2.97 Al-Al = 2.80	edge: trigonal planar clusters of Mg-Mg and Mg-Al $\perp c$; infinite spiral clusters of Al-Al $\parallel c$; substitutional blocking by Mg^{2+} and Al^{3+}	Buerger et al 1962

Table 2 (*continued*)

Mineral (formula)	Sites (coord. no.)	M-M distances (Å)	Polyhedral linkages (type of sharing; extent of M-M cluster)	References
yoderite $(Al,Mg,Fe,Mn)_8$ $Si_4O_{18}(OH)_2$	Al_1 (6) Al_2 (5) Al_3 (5)	Al_1-Al_1 = 2.90 Al_1-Al_2 = 3.50 Al_1-Al_3 = 3.28	edge: infinite Al_1-Al_1 chains; isolated Al_1-Al_2 and Al_1-Al_3 clusters; substitutional blocking by Mg^{2+} & Al^{3+}	Fleet & Megaw 1962
orthopyroxenes $(Mg,Fe)_2Si_2O_6$	M1 (6) M2 (6)	M1-M1 = 3.15 M1-M2 = 3.08 and 3.27	infinite M1-M1 and M1-M2 chains ‖c; substitutional blocking by Mg^{2+}	Burnham et al 1971
augite $Ca(Mg,FeAl)(Si,Al)_2O_6$	M1 (6) M2 (8)	M1-M1 = 3.11 M1-M2 = 3.21	same as orthopyroxene	Clark et al 1969
Allende fassaite $Ca(Mg,Ti^{3+},Ti^{4+},Al)(Si,Al)_2O_6$	M1 (6)	M1-M1 = 3.15	same as augite	Dowty & Clark 1973a
Angra dos Reis fassaite $(Ca,Fe^{2+})(Fe^{2+},Ti^{4+},Mg,Al)(Si,Al)_2O_6$	M1 (6)	M1-M1 = 3.13	same as augite	Hazen & Finger 1977
omphacite $(Na,Ca)(Al,Fe,Ti)Si_2O_6$	M1 (6)	M1-M1 = 2.90	similar to orthopyroxene	Curtis et al 1975

glaucophane $Na_2(Mg,Fe^{2+})_3$ $(Al,Fe^{3+})_2Si_8$ $O_{22}(OH)_2$	M1 (6) M2 (6) M3 (6) M4 (8)	M1-M1 = 3.22 M1-M2 = 3.09 M1-M3 = 3.10 M2-M3 = 3.31 M2-M4 = 3.15 M1-M4 = 3.31	infinite bands of edge-shared octahedra ‖c; substitutional blocking by Mg^{2+} and Al^{3+}	Papike & Clark 1968
riebeckite, crocidolite $Na_2Fe_3^{2+}Fe_2^{3+}$ $Si_8O_{22}(OH)_2$	as for glaucophane	comparable to glaucophane	infinite bands of edge-shared $[FeO_6]$ octahedra	Hawthorne 1976
actinolite-hornblende $Ca_2(Mg;Fe,Al)_5$ $(Si,Al)_8O_{22}(OH)_2$	as for glaucophane	M1-M1 = 3.23 M1-M2 = 3.11 M1-M3 = 3.10 M2-M3 = 3.20 M2-M4 = 3.20 M1-M4 = 3.42	similar to glaucophane	Mitchell et al 1971
biotite (annite-phlogopite) $K(Mg,Fe^{2+},Fe^{3+})_{2-3}$ $(Si_3AlO_{10})(OH)_2$	M1 (6) M2 (6)	M1-M1 and M1-M2 ≈ 3.10–3.20	infinite 2-D sheets of edge-shared octahedra	Hazen & Burnham 1973
babingtonite $Ca_2Fe^{2+}Fe^{3+}Si_5O_{14}$ (OH)	Fe_1 (6) Fe_2 (6)	Fe_1-Fe_1 = 3.37 Fe_1-Fe_2 = 3.30	clusters of edge-shared $[FeO_6]$ octahedra four octahedra wide	Araki & Zoltai 1972 Kosoi 1976
ilvaite $CaFe_2^{2+}Fe^{3+}Si_2O_8(OH)$	Fe_A (6) Fe_B (6)	Fe_A-Fe_A = 2.83 and 3.03 (‖c) and 3.01 (⊥c), Fe_A-Fe_B = 3.15 and 3.25	infinite double chains of edge-shared Fe_A octahedra ‖c	Beran & Bittner 1974 Haga & Takéuchi 1976
deerite $Fe_6^{2+}Fe_3^{3+}O_3(Si_6O_{17})$ $(OH)_5$	cations in nine octahedral sites	range of M-M distance 3.11–3.31	infinite bands, six octahedra wide, of edge-shared $[FeO_6]$ octahedra	Fleet 1977

Table 2 (*continued*)

Mineral (formula)	Sites (coord. no.)	M-M distances (Å)	Polyhedral linkages (type of sharing; extent of M-M cluster)	References
howieite $NaFe^{2+}_{10}Fe^{3+}_{3}(Si_{12}O_{34})(OH)_{10}$	cations in six octahedral sites	range of M-M distance 3.16–3.29	infinite bands, four octahedral wide of edge-shared $[FeO_6]$ octahedra	Wenk 1974
sapphirine $(Mg,Fe^{2+},Al,Fe^{3+})_7(Si,Al)_6O_{20}$	cations in seven octahedral sites	range of M-M distance 3.18–3.35	infinite bands, four and three octahedral wide of edge-shared octahedra	Moore 1969 Higgins et al 1979 Higgins & Ribbe 1979 Merlino 1980
aenigmatite $Na_2Fe_5TiSi_6O_{20}$	similar to sapphirine	comparable to sapphirine	similar to sapphirine	Cannillo et al 1971
magnetite Fe_3O_4	Fe_A (4) Fe_B (6)	Fe_B-Fe_B = 2.97 Fe_A-Fe_B = 3.48	infinite single chains of edge-shared $[FeO_6]$ running in 3-D	Hamilton 1958
Ti andradite (schorlomite) $(Ca,Fe^{2+})_3(Fe^{3+},Fe^{2+},Ti^{4+},Ti^{3+},Al)_2(Si,Fe^{3+},Al)_3O_{12}$	{X} (8) [Y] (6) (Z) (4)	X-Z = 3.01 X-Y = 3.37 Y-Z = 3.37	edge: chains of $\{XO_8\}$ cubes and (ZO_4) tetrahedra; corner-shared $[YO_6]$ octahedra and (ZO_4) or $\{XO_8\}$	Novak & Gibbs 1971

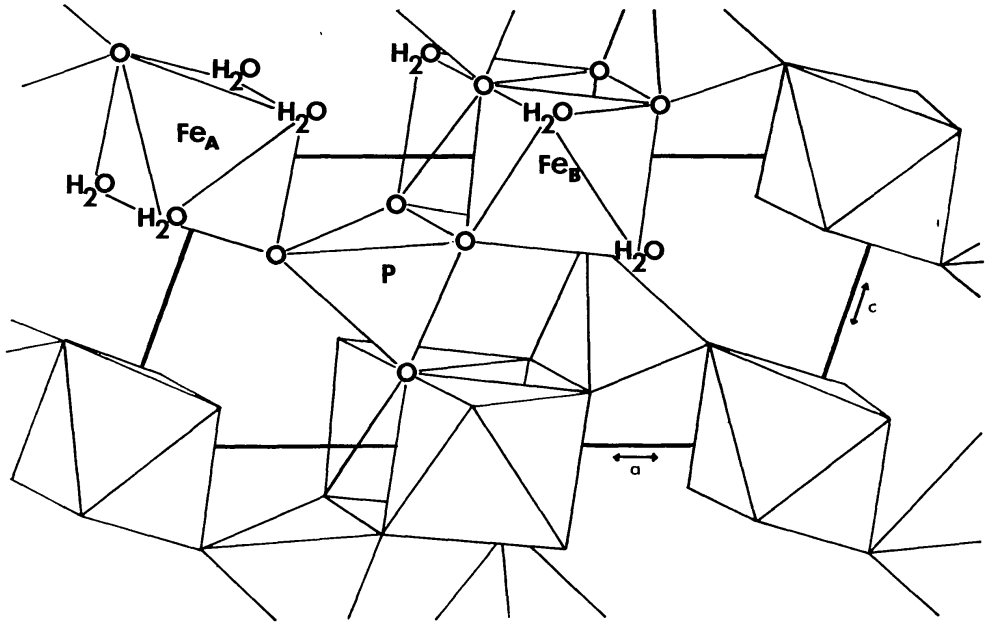

Figure 1 The vivianite crystal structure viewed along the *b* axis.

The crystal structure of vivianite illustrated in Figure 1 contains two distinct octahedral sites, designated Fe_A and Fe_B. The Fe_A octahedra are isolated, but pairs of Fe_B octahedra share a common edge across which the Fe^{2+} ions are separated by only 2.85 Å along the *b* axis. Polarized absorption spectra of vivianites (Hush 1967, Faye et al 1968) show an intense absorption band centered at 15,200 cm^{-1} when light is polarized along the *b* axis (the Fe_B-Fe_B direction) which effectively masks all but blue light when radiation is transmitted through the crystals. The polarization dependence of the 15,200 cm^{-1} band is the key to its assignment; it originates from a $Fe^{2+} \rightarrow Fe^{3+}$ intervalence transition between adjacent Fe^{2+} and Fe^{3+} ions in the edge-shared Fe_B octahedra. The intensity of this charge transfer band increases significantly with decreasing temperature (Smith & Strens 1976) and rising pressure (Mao 1976), supporting its assignment as an intervalence transition between Fe^{2+} and Fe^{3+} ions.

Inherent in this assignment, however, are the assumptions that Fe^{3+} ions are present and that some occur in the Fe_B sites, which are not implied by the stoichiometry of vivianite. Confirmation comes from recent Mössbauer measurements of vivianites (McCammon & Burns 1980). The Mössbauer spectra of samples mechanically ground in air, such as the profiles illustrated in Figure 2, show that Fe^{2+} ions in both Fe_A and Fe_B octahedra are oxidized to Fe^{3+} ions. However, Fe_A^{2+}/Fe_B^{2+} ratios increase with rising Fe^{3+} concentration, suggesting that there is a greater probability of oxidizing remaining Fe_A^{2+} ions than the second Fe^{2+} ion of a Fe_B^{2+}-Fe_B^{3+} pair.

Vivianite has the potential of being a Class IIIA mixed-valence compound with respect to the Fe_B octahedra. However, the Mössbauer spectra measured as high as the thermal decomposition temperature of vivianite (56°C) resolve only octahedral Fe^{2+} and Fe^{3+} ions indicating that individual iron cations have discrete valencies in the vivianite structure. Thus, although $Fe^{2+} \rightarrow Fe^{3+}$ intervalence transitions occur when light is polarized along the short Fe_B-Fe_B axis, the electron exchanged between each Fe_B^{2+}-Fe_B^{3+} pair is effectively localized on an individual

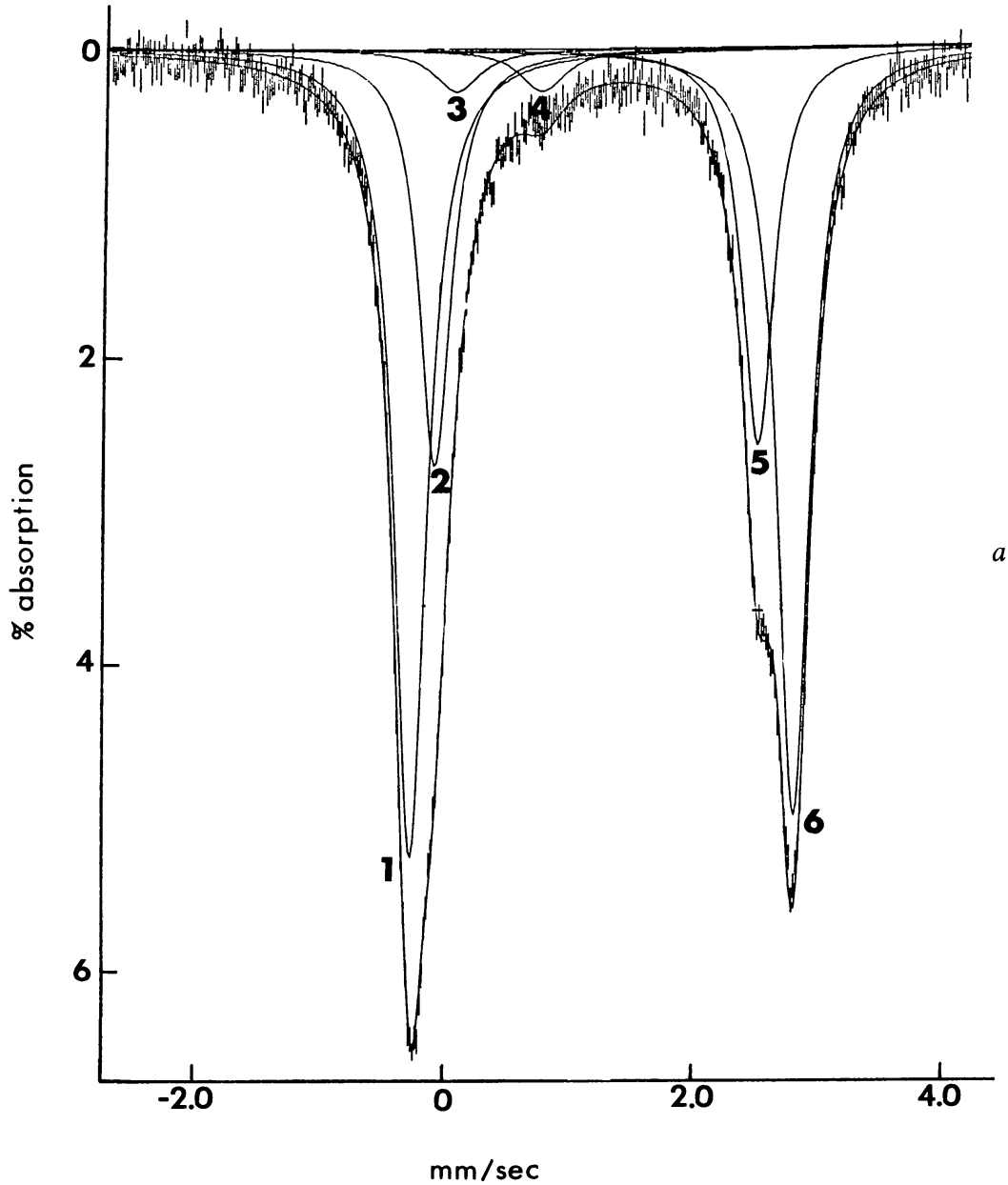

Figure 2 Mössbauer spectra of vivianite (*a*) before and (*b*) after oxidation by mechanical grinding in air. Peaks 1 and 6: Fe^{2+} in the Fe_B sites; peaks 2 and 5: Fe^{2+} in the Fe_A sites; peaks 3 and 4: octahedral Fe^{3+}. From McCammon & Burns (1980).

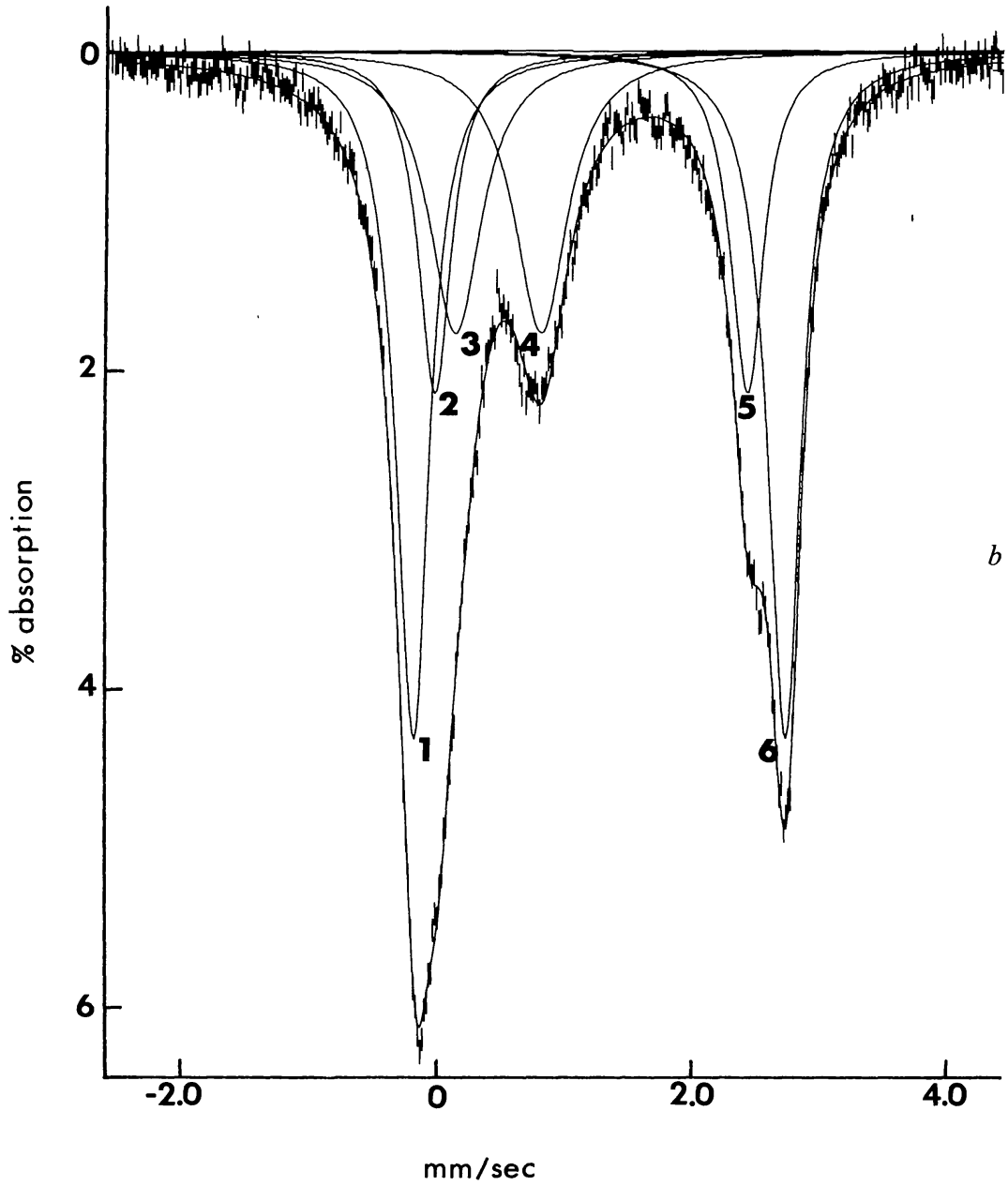

Figure 2 (*continued*)

cation during the lifetime (10^{-7} s) of the Mössbauer transition. Vivianite is thus a Class II mixed-valence compound.

Magnetite

Another mineral cited as a typical example of a mixed-valence compound (Robin & Day 1967, Day 1976) is magnetite, Fe_3O_4 or $Fe^{2+}Fe_2^{3+}O_4$. It is considered to be a Class IIIB mixed-valence compound because the magnetite structure contains infinite chains of Fe^{2+}-Fe^{3+} octahedra exhibiting electron delocalization. However, a phase change in magnetite at

119 K complicates interpretations of electron delocalization in this structure type.

The magnetite structure, an inverse spinel, contains Fe^{3+} ions in tetrahedral A sites, and Fe^{2+} and Fe^{3+} ions separated by 2.97 Å in three-dimensional infinite chains of edge-shared octahedral B sites extending along [100] directions. Above 119 K, electron delocalization involving the B-site cations occurs in magnetite, resulting in opacity and high electrical and thermal conductivities. The Mössbauer spectra show two cation species: tetrahedral Fe^{3+} and mixed-valence octahedral iron (Sawatzky et al 1969, Lotgering & Diepen 1977, Kundig & Hargrove 1969). At 119 K a phase change occurs (Hamilton 1958) which doubles the unit cell, leads to magnetic ordering of Fe^{2+} and Fe^{3+}, and produces distinguishable Fe^{2+} and Fe^{3+} in octahedral sites with attendant drop in electrical conductivity and changes in the Mössbauer spectra (Verwey & Haayman 1941, Verble 1974). The transition in magnetite, which is called the Verwey transition, is interpreted as an ionic order-disorder transition, but controversy has arisen recently concerning the number of disordering parameters necessary and the validity of the order-disorder model versus a band model or polaron model (Cullen & Callen 1971, Verble 1974). Thus, although magnetite is classified as the type-example of a Class IIIB mixed-valence compound, application of a Verwey-type model of quenched electron delocalization to other systems not showing a phase change should be made with caution.

Ilvaite

Many of the attributes of electron delocalization in a mixed-valence compound are displayed by ilvaite, $CaFe_2^{2+}Fe^{3+}Si_2O_8(OH)$. The ilvaite structure, which is illustrated in Figure 3, consists of a framework of infinite double chains of edge-shared Fe(A) octahedra linked by corner-shared double tetrahedral Si_2O_7 groups. Six-coordinated Fe(B) sites and seven-coordinated Ca sites are bonded to oxygens of this framework. Neutron diffraction measurements have demonstrated that Fe^{2+} and Fe^{3+} ions are located in the Fe(A) sites while Fe(B) sites accomodate Fe^{2+} ions (Haga & Takéuchi 1976). Many $Fe^{2+} \rightarrow Fe^{3+}$ interactions are possible between the edge-shared octahedra shown in Figure 4. Thus, Fe(A)-Fe(A) couples occur along the chains in the *c* direction (Fe-Fe distances of 2.83 Å and 3.03 Å), and across the chain in the *a-b* plane (Fe-Fe = 3.01 Å). Four Fe(B) → Fe(A) interactions occur per Fe(B) site with Fe-Fe distances ranging from 3.15 Å to 3.25 Å.

Electron delocalization behavior has been deduced from the temperature variations of the Mössbauer spectra of ilvaite (Gérard & Grandjean 1971, Grandjean & Gérard 1975, Nolet 1978, Nolet & Burns 1979). The spectral profiles show significant variations between 80 K and 390 K (for

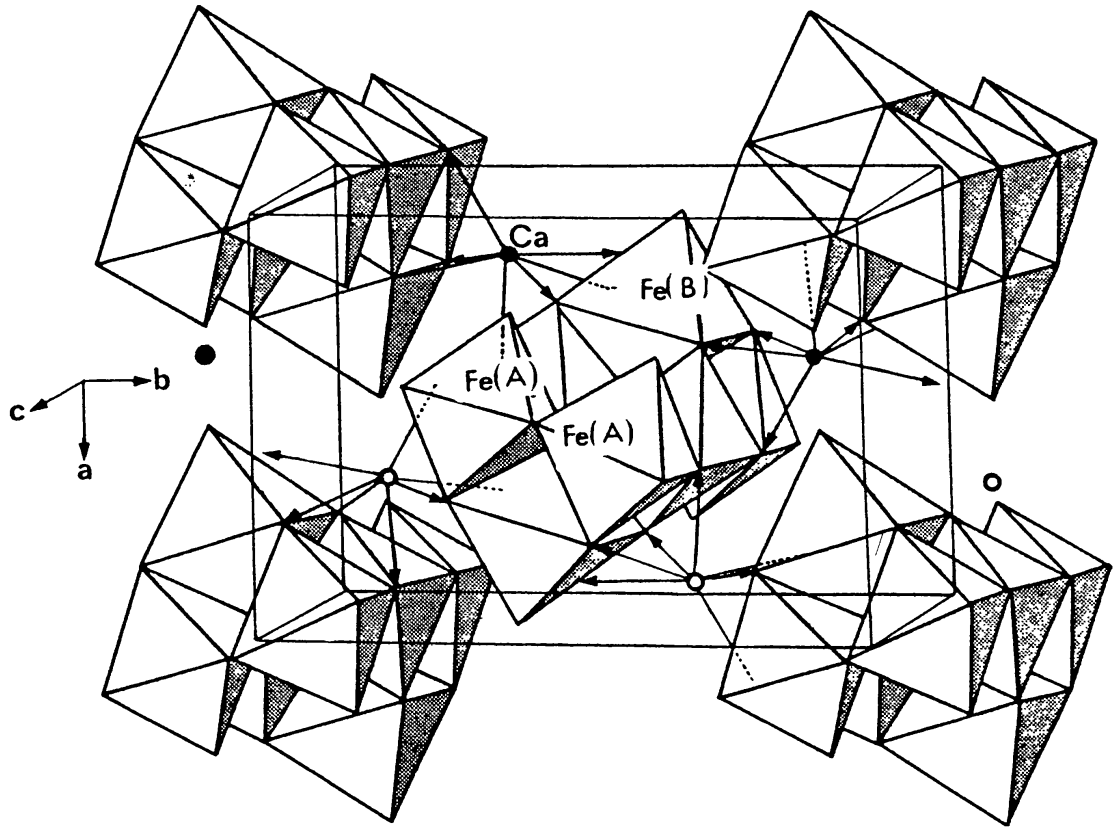

Figure 3 The ilvaite crystal structure, showing the arrangement of infinite double chains of edge-shared Fe(A) octahedra extending along the *c* axis. From Nolet & Burns (1979).

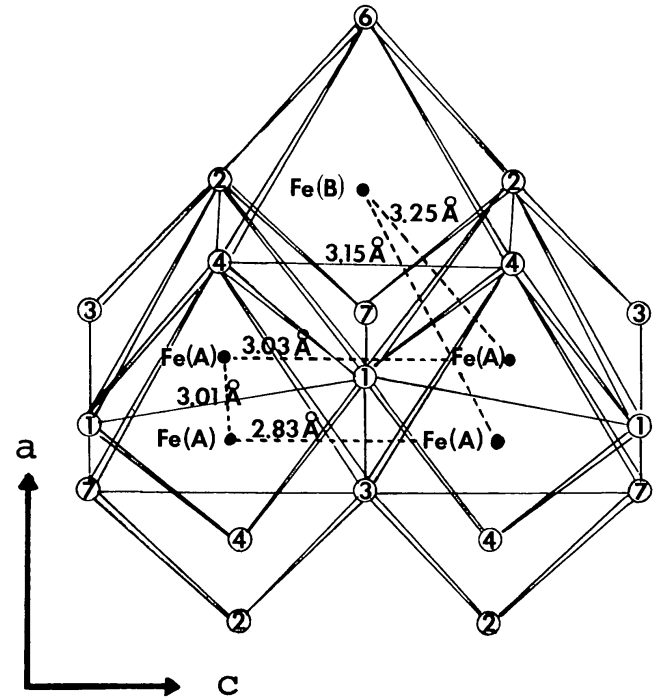

Figure 4 Projection of one unit of the Fe(A) double chain showing possible Fe(A)-Fe(A) and Fe(A)-Fe(B) interactions across shared edges and appropriate metal-metal distances. From Nolet & Burns (1979).

example, see Figure 5) which was earlier attributed to a Verwey-type transition in ilvaite at about 320 K. Recently, the Mössbauer spectra of a suite of ilvaite specimens were successfully fitted to five component doublets (Nolet & Burns 1979), the assignments of which are shown in Figure 5. In addition to one doublet for octahedral Fe^{3+} and two Fe^{2+} doublets representing cations in the Fe(A) and Fe(B) sites, two additional doublets were resolved representing delocalized $[Fe^{2+}(A) \rightarrow Fe^{3+}(A)]$ species parallel to and perpendicular to the chains of edge-shared Fe(A) octahedra (Figure 4). The latter two assignments explain the strong absorption and dark colors of ilvaite in all crystallographic directions. The temperature variations of the ilvaite Mössbauer spectra are therefore not due to a localized-delocalized order-disorder transition, but rather to conditions where peaks due to $[Fe^{2+}(A) \rightarrow Fe^{3+}(A)]$ delocalized species become resolvable at elevated temperatures. Certain electronic levels associated with discrete valencies become depopulated with increasing temperature contemporaneous with population of new delocalized levels associated with intermediate valencies.

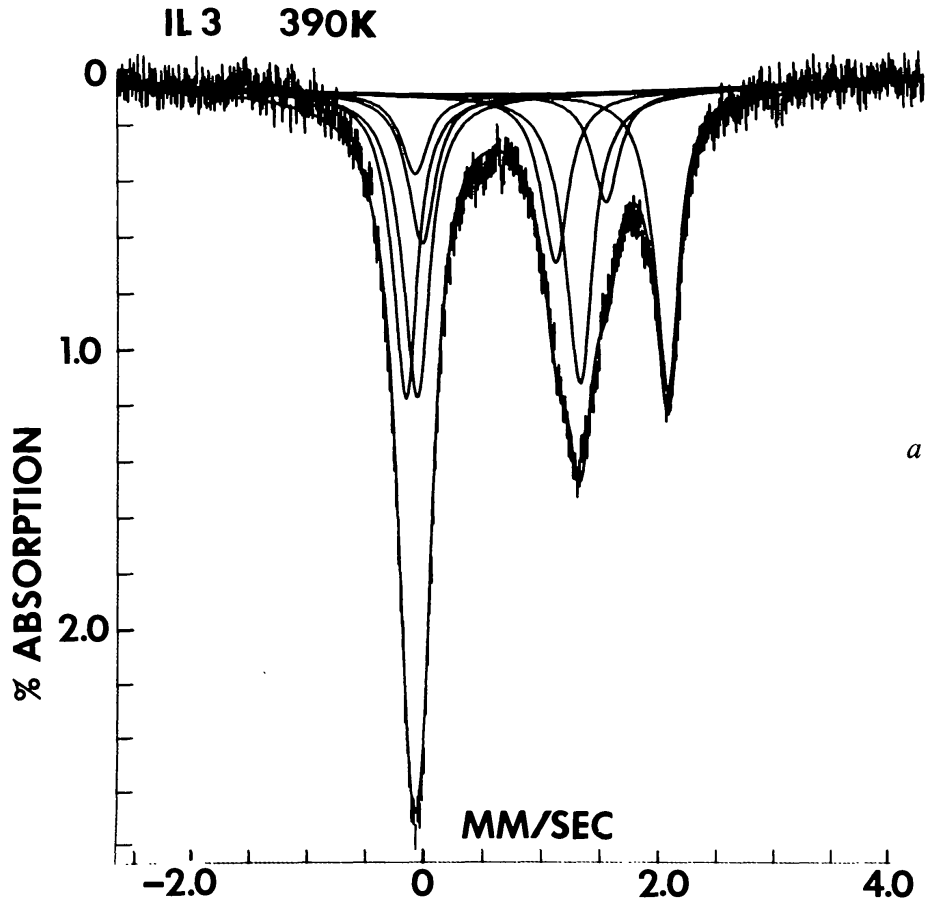

Figure 5 Fitted Mössbauer spectra for ilvaite specimen IL3: (*a*) the 390 K spectrum fitted to eight peaks or four doublets, $Fe^{2+}(A)$ is below resolution of spectrometer; (*b*) the 80 K spectrum showing assignments of component doublets. From Nolet & Burns (1979).

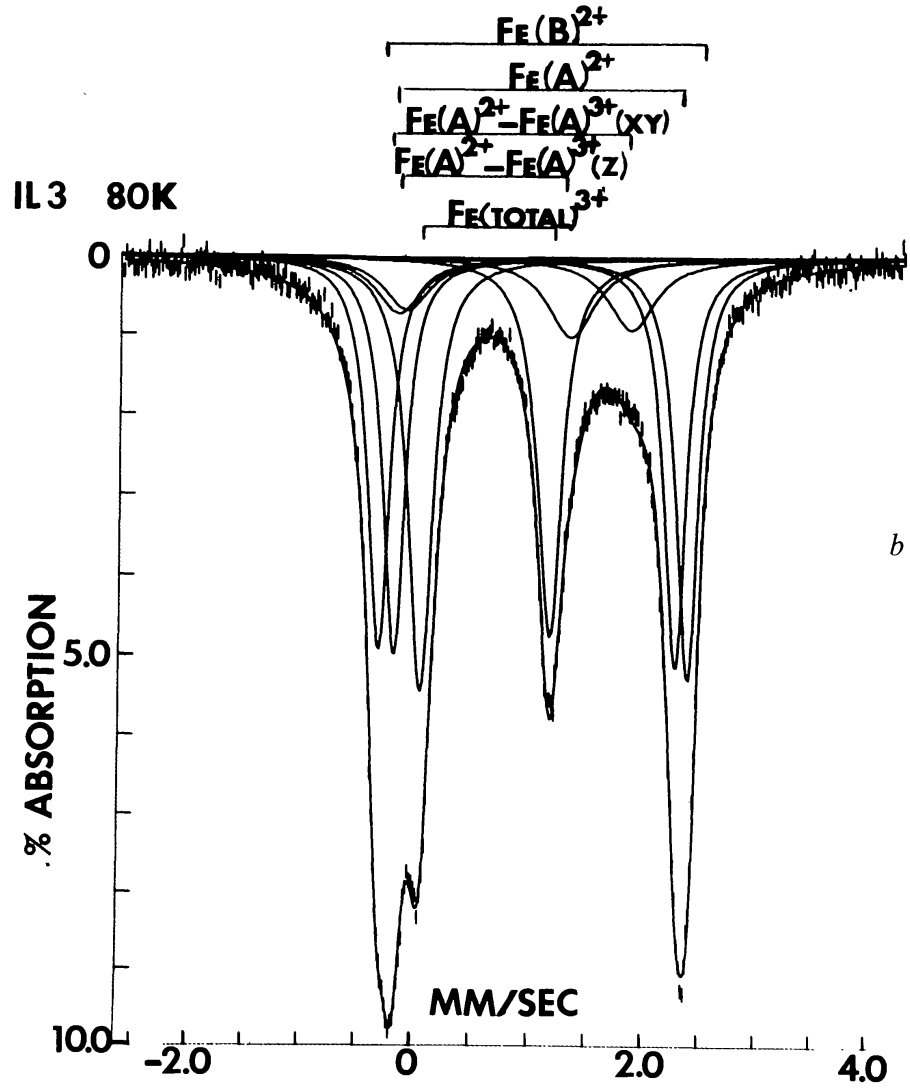

Figure 5 (*continued*)

The effect of pressure to 60 kb on the Mössbauer spectra of ilvaite are similar to temperature, but are highly orientation dependent (Evans & Amthauer 1980). Thus, the emergence of delocalized [Fe^{2+}(A) → Fe^{3+}(A)] species is most pronounced for sections cut parallel to (001), in which the compression axis is *c*, corresponding to the direction of infinite chains of linked octahedra (Figure 3).

Ilvaite with its infinite chains of edge-shared Fe^{2+}-Fe^{3+} octahedra is a model example of a Class IIIB mixed-valence compound with respect to the Fe(A) octahedra. The short Fe(A)-Fe(A) distances, 2.83–3.03 Å, are particularly conducive to electron delocalization. The Fe(A)-Fe(B) octahedral clusters, however, constitute a Class II compound, the somewhat larger Fe(A)-Fe(B) distances (3.15–3.25 Å) being less conducive to electron delocalization. Ilvaite is representative of several end-member Fe^{2+}-Fe^{3+} silicate minerals in which electron delocalization is predicted

or observed along chains of linked octahedra. Further examples are discussed below.

Deerite

Another mixed-valence mineral recently demonstrated by Mössbauer spectroscopy to exhibit electron delocalization is deerite, $Fe_6^{2+}Fe_3^{3+}O_3Si_6O_{17}(OH)_5$. The crystal structure of this chain silicate mineral contains bands of edge-shared octahedra, six octahedra wide, extending along the *c* axis (Fleet 1977). Although the structure contains nine distinct Fe atom positions, they are grouped into three sets of three virtually equivalent octahedral sites. The Fe-Fe distances across the edge-shared octahedra range from 3.10 Å to 3.31 Å. By analogy with ilvaite, the profiles of the Mössbauer spectra of deerite are strongly temperature dependent (Frank & Banbury 1974, Amthauer et al 1980). The spectra indicate that at 77 K discrete Fe^{2+} and Fe^{3+} ions exist in deerite, but at 298 K about 20% of the iron cations take part in thermally activated electron delocalization processes across the edge-shared octahedra (Amthauer et al 1980).

Babingtonite

Babingtonite, $Ca_2Fe^{2+}Fe^{3+}Si_5O_{14}(OH)$, has a formula resembling ilvaite and deerite and might be expected to display electron delocalization. Edge-shared octahedra also occur in the babingtonite structure. However, they do not form infinite chains as exist in ilvaite and deerite. There are two distinct Fe sites in babingtonite, designated Fe(1) and Fe(2), and clusters of edge-shared Fe(2)-Fe(1)-Fe(1)-Fe(2) octahedra, four wide, link two chains of corner-shared SiO_4 tetrahedra (Araki & Zoltai 1972). The Fe(2)-Fe(1) and Fe(1)-Fe(1) distances are about 3.30 Å and 3.37 Å, respectively, and average Fe-O distances are approximately 2.17 Å and 2.05 Å, respectively, leading to the assignment of Fe^{2+} and Fe^{3+} ions in the larger Fe(1) and smaller Fe(2) octahedra, respectively. Mössbauer measurements between 30 K and 600 K confirmed this highly ordered cation distribution and failed to detect any electron-delocalized iron cation species (Amthauer 1980). Babingtonite, therefore, resembles vivianite by containing discrete Fe^{2+} and Fe^{3+} ions. Evidently, the limited extent of edge-shared octahedra and large Fe-Fe distances are not conducive to electron delocalization behavior in babingtonite.

Glaucophane-Riebeckite

Ilvaite and deerite represent end-member mixed-valence silicates the crystal structures of which contain infinite chains of edge-shared $[FeO_6]$ octahedra permitting electron delocalization. Several other silicate minerals also have structures in which infinite chains of edge-shared octahe-

dra exist, but atomic substitution of non–transition metal ions such as Mg^{2+} and Al^{3+} with ionic radii similar to those of Fe^{2+} and Fe^{3+} limit the extent of $Fe^{2+} \rightarrow Fe^{3+}$ interactions by substitutional blocking.

The model mineral showing intervalence transitions and substitutional blocking of electron delocalization is glaucophane, $Na_2(Mg,Fe^{2+})_3(Al,Fe^{3+})_2Si_8O_{22}(OH)_2$. The Fe^{2+}-Fe^{3+} end-member mineral is riebeckite, $Na_2Fe_3^{2+}Fe_2^{3+}Si_8O_{22}(OH)_2$, the asbestiform variety of which is called crocidolite. The glaucophane structure, like other amphiboles, contains bands of octahedral sites, designated M1, M2, and M3, two or three octahedra wide, extending along the *c* axis (Papike & Clark 1968). In highly ordered blue-schist facies glaucophanes, the larger M1 and M3 octahedra are occupied preferentially by Mg^{2+} and Fe^{2+} ions, while the smaller Al^{3+} and Fe^{3+} ions are enriched in the smaller M2 octahedra. Metal-metal distances across the edge-shared octahedra are in the range 3.09–3.31 Å. Intervalence $Fe^{2+} \rightarrow Fe^{3+}$ transitions, primarily $Fe^{2+}(M1) \rightarrow Fe^{3+}(M2)$ and $Fe^{2+}(M3) \rightarrow Fe^{3+}(M2)$, account for the blue-violet pleochroism of glaucophane and the polarization dependence of the absorption bands in the region 16,130–18,520 cm^{-1} when light is polarized only in the plane of edge-shared octahedra (Burns 1970). Similar charge transfer bands have been measured in the optical spectra of several alkali amphiboles and shown to have intensities proportional to the product of donor Fe^{2+} and acceptor Fe^{3+} concentrations (Littler & Williams 1965, Smith & Strens 1976). A similar concentration dependence was found for the electrical conductivity of crocidolite (Littler & Williams 1965) which is significantly high along the fiber axis (the direction of infinite chains of edge-shared $[FeO_6]$ octahedra).

Although the amphibole structure is conducive to electron delocalization by having short enough metal-metal distances and infinite chains of edge-shared octahedra, the Mössbauer spectra of several compositions along the glaucophane-riebeckite solid solution series have resolved only doublets attributable to discrete Fe^{2+} and Fe^{3+} cations. Negligible electron delocalization in glaucophane is certainly attributable to Mg^{2+} and Al^{3+} blocking $Fe^{2+} \rightarrow Fe^{3+}$ interactions along the chains of edge-shared octahedra. In the riebeckite end-member composition, however, electron delocalization may also be limited by the slightly larger Fe-Fe distances (compared to ilvaite and magnetite) and dissimilarities between the M1, M2, and M3 octahedra which render alkali amphiboles Class II mixed-valence compounds. Riebeckite might acquire electron delocalization detectable by the Mössbauer effect if cations were more randomly distributed in the crystal structure. Such disordering may account for the unusually high electrical conductivity of heated crocidolites (Littler & Williams 1965), while additional peaks in the Mössbauer spectra of

pegmatitic riebeckites (Bancroft & Burns 1969) might represent delocalized $Fe^{2+} \rightarrow Fe^{3+}$ species instead of Fe^{2+} ions disordered into M2 sites.

Other Examples

Substitutional blocking typified by glaucophane is an important factor controlling the electronic properties of minerals. Several iron-bearing silicates contain infinite chains, bands, or sheets of edge-shared octahedra, but electron delocalization is prevented by atomic substitution of Mg^{2+} and Al^{3+} in solid solution series which block extended $Fe^{2+} \rightarrow Fe^{3+}$ interactions. However, intense intervalence bands are frequently observed in polarized spectra of such minerals measured in the visible region. Examples of minerals showing discrete valencies for Fe^{2+} and Fe^{3+} ions as a result of atomic substitution, to which $Fe^{2+} \rightarrow Fe^{3+}$ intervalence transitions across edge-shared octahedra have been assigned, are listed in Table 3. They include micas of the phlogopite-biotite series, amphiboles of the actinolite-hornblende series, many pyroxenes, omphacite, certain tourmalines, chlorite, kyanite, and potentially sapphirine.

On the other hand, end-member Fe^{2+}-Fe^{3+} silicates expected to display electron delocalization behavior, in addition to deerite, ilvaite, and perhaps riebeckite, include howieite, aenigmatite, annite, and stilpnomelane.

$Fe^{2+} \rightarrow Fe^{3+}$ INTERACTIONS IN OTHER COORDINATION SYMMETRIES

The majority of mixed-valence iron-bearing minerals displaying $Fe^{2+} \rightarrow Fe^{3+}$ interactions contain cations in edge-shared octahedra. However, intervalence transitions and electron delocalization behavior have been documented between iron cations in other coordination symmetries.

Cordierite

The best known example of Fe^{2+}(octahedral) $\rightarrow$ Fe^{3+}(tetrahedral) interactions is in the mineral cordierite, $Al_3(Mg,Fe^{2+})_2[(Al,Fe^{3+})Si_5O_{18}]$. The crystal structure of cordierite contains M octahedra which share edges with two T_1 and one T_2 tetrahedra (Gibbs 1966). The Fe^{3+} ions are believed to be concentrated in the T_1 tetrahedra, while Fe^{2+} ions occupy M octahedra. The M-T_1 distances across the isolated M octahedron-T_1 tetrahedron clusters is only 2.74 Å. The absorption spectra of cordierite show a broad intense band at about 17,000 cm^{-1} polarized in the plane of the edge-shared M and T_1 polyhedra, the intensity of which increases at low temperatures (Smith & Strens 1976, Faye et al 1968, Goldman & Rossman 1978). The Mössbauer spectra of such cordierites, however, show

Table 3 Spectral data for mixed-valence minerals of Fe and Ti

Mineral	CT energy (cm^{-1}) and assignment	Comments (Möss. spect.; elect. cond.; T variations, etc)	References
vivianite	15,200: $Fe_B^{2+} \rightarrow Fe_B^{3+}$	M/S spectra: discrete valencies; inverse T depend. of intensity of CT; P intensifies CT.	Hush 1967, Faye et al 1968, Smith & Strens 1976, Mao 1976, McCammon & Burns 1980
sapphire	17,000 ($\perp$c): $Fe^{2+} \rightarrow Ti^{4+}$ 11,150 ($\perp$c): $Fe^{2+} \rightarrow Ti^{4+}$ 12,900 (||): $Fe^{2+} \rightarrow Fe^{3+}$ 9,700 (||c): $Fe^{2+} \rightarrow Fe^{3+}$	No M/S; inverse T depend. of CT; debate over assignment	Townsend 1968, Lehmann & Harder 1970, Faye 1971, Ferguson & Fielding 1972, Eigenmann et al 1972, Smith & Strens 1976, Smith 1978b
kyanite	16,500: $Fe^{2+} \rightarrow Ti^{4+}$ 11,500: $Fe^{2+} \rightarrow Fe^{3+}$	M/S confirms Fe^{2+}; inverse T dependence of CT; debate over assignment	White & White 1967, Faye & Nickel 1969a, Faye 1971, Smith & Strens 1976, Parkin et al 1977
aquamarine (beryl)	16,100 (||c): $Fe^{2+} \rightarrow Fe^{3+}$	M/S confirms Fe^{2+}; debate over assignment	Wood & Nassau 1968, Loeffler & Burns 1976, Parkin et al 1977, Goldman et al 1978
cordierite (iolite)	17,500 ($\perp$c): $Fe_M^{2+} \rightarrow Fe_{T_1}^{3+}$	M/S detects Fe^{3+} at 77 K only; inverse T dependence of CT	Farrell & Newnham 1967, Faye et al 1968, Smith & Strens 1976, Pollak 1976, Parkin et al 1977; Goldman et al 1978
osumilite	15,480 cm^{-1}($\perp$c): Fe^{2+}(oct) $\rightarrow$ Fe^{3+}(tet); or Fe^{2+}(oct) $\rightarrow$ Fe^{3+}(channel)	M/S detects Fe^{2+} in oct. and channel sites; Fe^{3+} in tet.; discrete valencies	Faye 1972, Goldman & Rossman 1978
tourmaline	18,000 ($\perp$c $\gg$ ||c): Fe^{2+}(Mg) $\rightarrow$ Fe^{3+}(Mg,Al)	M/S detects Fe^{2+} in Mg and Al sites; discrete valencies; inverse T dependence of CT; considerable debate over assignment	Faye et al 1968, Townsend 1970, Wilkins et al 1969, Burns 1972, Hermon et al 1973, Faye et al 1974, Smith & Strens 1976, Smith 1977, 1978a

Table 3 (*continued*)

Mineral	CT energy (cm^{-1}) and assignment	Comments (Möss. spect.; elect. cond.; T variations, etc)	References
yoderite	13,800: $Fe^{2+}(Al_1) \rightarrow Fe^{3+}(Al_1)$ 16,500: $Mn^{2+}(Al_1) \rightarrow Mn^{3+}(Al_1)$ 21,000: $Mn^{2+}(Al_1) \rightarrow Mn^{3+}(Al_1)$	M/S detects Fe^{2+} and Fe^{3+}: discrete valencies	Abu-Eid et al 1978
orthopyroxenes	14,500 (||c): Fe^{2+}(M2,M1) $\rightarrow Fe^{3+}$ (M1)	M/S detects Fe^{2+} and Fe^{3+}; Fe^{2+} strongly ordered in distorted M2 site	Burns 1970, Burnham et al 1971, Goldman & Rossman 1977a, Annersten et al 1978
augite	13,000: $Fe^{2+}_{M1} \rightarrow Fe^{3+}_{M1}$	M/S detects Fe^{2+} and Fe^{3+}; discrete valencies	Burns et al 1976
Allende fassaite	16,000: $Ti^{3+}_{M1} \rightarrow Ti^{4+}_{M1}$	P intensifies CT, but negligible shift in energy	Dowty & Clark 1973a,b, Burns & Huggins 1973, Mao & Bell 1974
Angra dos Reis fassaite	20,6000: $Fe^{2+}_{M1} \rightarrow Ti^{4+}_{M1}$	M/S detects Fe^{2+} only; P intensifies CT and shifts to lower energy	Bell & Mao 1976, Mao et al 1977, Hazen et al 1977
omphacite	15,040: $Fe^{2+} \rightarrow Fe^{3+}$ or $Fe^{2+} \rightarrow Ti^{4+}$	Blue Ti variety; M/S detects Fe^{2+} and Fe^{3+} discrete valencies; P variations of position and intensity of CT	Abu-Eid 1976, Strens et al 1980, Aldridge et al 1978, Bancroft et al 1969
glaucophane	18,520 (||b): Fe^{2+}(M1,M3) $\rightarrow Fe^{3+}$(M2) 16,130 (||c): Fe^{2+}(M1) $\rightarrow Fe^{3+}$(M2)	M/S detects Fe^{2+} and Fe^{3+}; discrete valencies; Fe^{2+} ordered in M1 and M3; inverse T dependence of CT	Bancroft & Burns 1969, Ernst & Wai 1970, Smith & Strens 1976

riebeckite, crocidolite	15,000–18,000: $Fe^{2+} \rightarrow Fe^{3+}$	High elect cond.; M/S detects Fe^{2+} and Fe^{3+}; discrete valencies	Littler & Williams 1965, Hush 1967, Bancroft & Burns 1969, Manning & Nickel 1969, Faye & Nickel 1969b, Borg & Borg 1980
actinolite-hornblende	14,200 (||b) and 13,700 ($\perp$c): $Fe^{2+} \rightarrow Fe^{3+}$	M/S detects Fe^{2+} in M1, M2, M3, and oct. Fe^{3+}; discrete valencies	Burns 1970, Burns & Greaves 1971, Bancroft & Brown 1975, Goldman & Rossman 1977b, Goldman 1979
biotite (annite-phlogopite)	13,650 and 16,400: $Fe^{2+} \rightarrow Fe^{3+}$(M1 $\rightarrow$ M2 and M2 $\rightarrow$ M2)	M/S resolved into four doublets; Fe^{2+} and Fe^{3+} in M1 and M2; discrete valencies; inverse T dependence of CT	Faye 1968, Robbins & Strens 1972, Annersten 1974, Bancroft & Brown 1975, Smith & Strens 1976, Smith 1977, 1978b, Faye & Hogarth 1969
babingtonite	opaque—very dark green	M/S detects Fe^{2+} and Fe^{3+}, each on only one oct. site	Araki & Zoltai 1972, Amthauer 1980
ilvaite	green–dark brown	M/S detects discrete valencies Fe^{2+} in Fe_A and Fe_B, and Fe^{3+} in Fe_A; two ED species detected assigned to $Fe^{2}{}_{A}{}^{+} \rightarrow Fe^{3+}_{A}$ ||c and $\perp$c.	Gérard & Grandjean 1971, Grandjean & Gérard 1975, Heilmann et al 1977, Paques-Ledent et al 1977, Nolet 1978, Nolet & Burns 1978, 1979, Evans & Amthauer 1980, Yamanaka & Takéuchi 1979.
deerite	opaque	low mag. susc.; M/S detects discrete valencies Fe^{2+} and Fe^{3+} each in two or more oct. at least two ED species detected	Carmichael et al 1966, Bancroft et al 1968, Frank & Banbury 1974, Bancroft 1979, Amthauer et al 1980, Pollak et al 1979

Table 3 (*continued*)

Mineral	CT energy (cm^{-1}) and assignment	Comments (Möss. spect.; elect. cond.; T variations, etc)	References
howieite	dark-green; no electronic spectra	M/S detects discrete valencies Fe^{2+} and Fe^{3+} ions; evidence of some ED species	Bancroft et al 1968
sapphirine	blue-green; no electronic spectra	M/S detects discrete valencies Fe^{2+} and Fe^{3+}	Bancroft et al 1968
aenigmatite	dark-blue; no electronic spectra	M/S detects discrete valencies Fe^{2+} and Fe^{3+}	Osborne & Burns unpubl. results
magnetite	opaque	high elect. cond. above 119 K; M/S resolves Fe_A^{3+} (tet.) and ED species in Fe_B	Verwey & Haayman 1941, Sawatzky et al 1969, Kundig & Hargrove 1969, Verble 1974, Cullen & Callen 1971, Lotgering & van Diepen 1977
Ti garnet	5,280: $Fe^{2+}\{X\} \rightarrow Fe^{3+}(Z)$	M/S detects discrete valencies Fe^{3+} in [Y] and (Z), Fe^{2+} in {X} and [Y]; and ED species $Fe^{2+}\{X\} \rightarrow Fe^{3+}(Z)$; inverse T dependence of CT	Huggins et al 1977a,b, Amthauer et al 1977, Schwartz et al 1980, Moore & White 1971

no evidence of Fe^{3+} at room temperature, even in specimens reported to contain as much as 22% of the iron in the ferric state (Parkin et al 1977). It is only at 77 K that ferric iron is detected in the Mössbauer spectra, but then accounting for smaller proportions of the chemically analyzed Fe^{3+} ions. The failure to detect Fe^{3+} ions in the room temperature spectra might be explained if the electron transfer between adjacent Fe^{2+} and Fe^{3+} ions is faster than the Mössbauer transition. Ferric ions could appear in the 77 K spectra because electron hopping is partially quenched. The phenomena would be comparable to electron delocalization observed in magnetite and ilvaite in which $Fe^{2+} \rightarrow Fe^{3+}$ interactions produce species with Mössbauer parameters intermediate between those for discrete Fe^{2+} and Fe^{3+} ions. Such "averaging" is not observed in the room-temperature Mössbauer spectra of cordierite, however, even in specimens containing Fe^{3+}/total Fe ratios as high as 0.25 (Parkin et al 1977). Another possible explanation is that the $Fe^{2+} \rightarrow Fe^{3+}$ intervalence transition involves iron cations located in the channels enclosed by the hexagonal rings of corner-shared $[SiO_4]$ tetrahedra in the cordierite structure (Goldman et al 1977). Iron in a loosely bound channel site would have an anomalously low recoil-free fraction and not contribute to the room temperature Mössbauer spectra of cordierite. The problem remains unresolved at present.

Another example of $Fe^{2+} \rightarrow Fe^{3+}$ interactions between cations in octahedral and tetrahedral sites is osumilite which is related to cordierite. Here, the $Fe^{2+} \rightarrow Fe^{3+}$ intervalence transition occurs at 15,480 cm^{-1} and the room temperature Mössbauer spectra detect coexisting discrete Fe^{2+} and Fe^{3+} ions (Goldman & Rossman 1978, Faye 1972).

Fe-Ti Garnets

Garnets of the andradite-melanite-schorlomite series represent another mineral group containing Fe^{2+}-Fe^{3+} clusters of different coordination symmetries. Many andradites contain high titanium contents, leading to subsilicic compositions and unusual crystal chemistries of iron and titanium. In the garnet structure, $\{X\}$ cations are coordinated to eight oxygens at the vertices of a distorted cube. The $[Y]$ cations are octahedrally coordinated and (Z) cations are in tetrahedral coordination. The only edge-sharing interaction involves the $\{XO_8\}$ cubes. In particular, three-dimensional chains of edge-shared $\{XO_8\}$ cubes and (ZO_4) tetrahedra are present in the garnet structure, and in andradite the X-Z interatomic distance is only 3.01 Å (Novak & Gibbs 1971).

Mössbauer measurements of several titanium-bearing andradites (i.e. melanites and schorlomites) have revealed the presence of coexisting Fe^{2+} and Fe^{3+} ions, and have demonstrated that Fe^{3+} ions, and not Ti^{4+}, make up for the deficiencies of silicon in the tetrahedral sites (Burns

1972, Huggins et al 1977a,b, Schwartz et al 1980). Up to five component doublets have been fitted to the Mössbauer spectra, four of which may be unambigously assigned to Fe^{3+} ions in octahedral [Y] and tetrahedral (Z) sites and to Fe^{2+} ions in the cubic {X} and octahedral [Y] sites. A fifth doublet showing unusual temperature variations (Amthauer et al 1977) may be resolved in the Mössbauer spectra of Ti-rich garnets, and its assignment has aroused considerable debate. Its parameters are suggestive of tetrahedral Fe^{2+} ions (Amthauer et al 1977, Huggins et al 1977b), but the substitution of large Fe^{2+} ions in the small Si^{4+} sites is considered unlikely (Schwartz et al 1980), particularly when octahedral Fe^{3+} ions predominate. An alternative assignment of the fifth doublet to $[Fe^{2+}\{X\} \rightarrow Fe^{3+}(Z)]$ electron delocalization has been proposed (Schwartz et al 1980). This assignment argues against tetrahedral Fe^{2+} replacing Si^{4+} in the garnet structure, and also correlates with the short X-Z separation of 3.01 Å between edge-shared $\{XO_8\}$ cubes and (ZO_4) tetrahedra, as well as electronic spectral data. The near infrared spectra of titanian garnets show an absorption band at 5,280 cm^{-1} (Burns 1972, Huggins et al 1977b, Moore & White 1971), which was originally assigned to a crystal field transition in tetrahedral Fe^{2+} ions (Manning & Harris 1970). However, the temperature dependence of the 5,280 cm^{-1} band, which deceases in intensity with rising temperature (Moore & White 1971) is not consistent with a crystal field transition. Instead, it confirms with the temperature variations found for intervalence transitions in other minerals (Smith & Strens 1976, Smith 1977, 1978b). Furthermore, electrical conductivity measurements on garnets show that pure andradite is an insulator, but becomes a semiconductor as the Ti content increases (Moore & White 1971). The activation energy for conduction, estimated to be about 3,800 cm^{-1}, is close to the onset of the intervalence transition centered at 5,280 cm^{-1}. These results support the assignment of a doublet to a $[Fe^{2+}\{X\} \rightarrow Fe^{3+}(Z)]$ electron-delocalized species in the Mössbauer spectra of Fe-Ti garnets (Schwartz et al 1980).

Although the garnet structure contains infinite chains of edge-shared $\{XO_8\}$ cubes and (ZO_4) tetrahedra, the extent of $[Fe^{2+}\{X\} \rightarrow Fe^{3+}(Z)]$ interactions is limited by substitutional blocking because Ca^{2+} and Si^{4+} ions are the major constituents of the {X} and (Z) sites, respectively, of andradite. It has been suggested that the $[Fe^{2+}\{X\} \rightarrow Fe^{3+}(Z)]$ interaction is facilitated by the similar relative energy levels of t_{2g} (t_2) and e_g (e) molecular orbitals in cubic and tetrahedral coordinations (Schwartz et al 1980). The $\{XO_8\}$-(ZO_4) coordination clusters in the garnet structure suggest that this mineral should be a Class I mixed-valence compound (Table 1). However, the semiconductor and electron delocalization properties of $[Fe^{2+}\{X\} \rightarrow Fe^{3+}(Z)]$ clusters in Fe-Ti garnets detected by Mössbauer spectroscopy are more indicative of a Class IIIA compound.

MINERALS WITH Ti^{3+}-Ti^{4+} OCTAHEDRAL CLUSTERS

The Ti(III) oxidation state is rare in terrestrial minerals due to the comparatively high redox conditions on Earth. However, Ti^{3+} ions may exist in Fe-Ti garnets (Burns 1972, Huggins et al 1977b, Schwartz et al 1980) and in some high pressure phases in the Mantle (Burns 1976). Trivalent titanium does occur in extraterrestrial materials, however, including titanian pyroxenes and glasses from certain meteorites and the Moon (Burns et al 1972, Sung et al 1974, Bell et al 1976, Dowty & Clark 1973a).

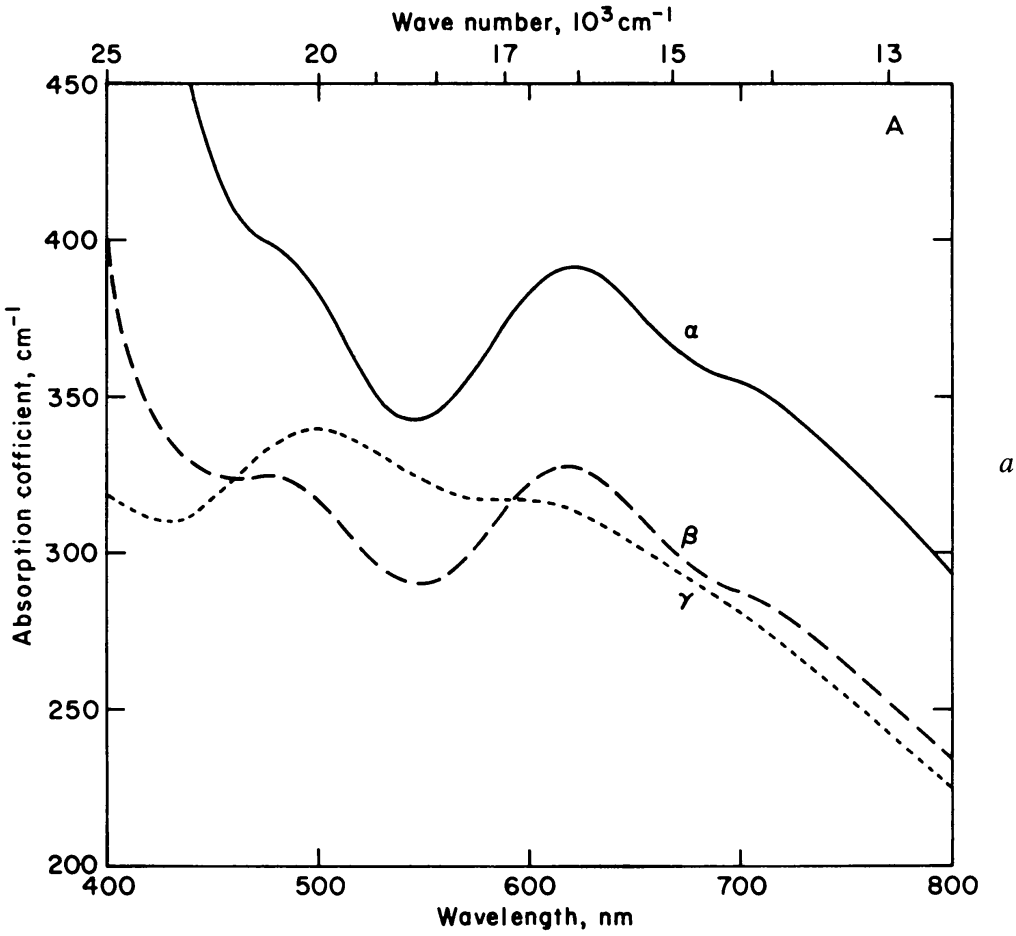

Figure 6 Spectra of the Ti^{3+}-Ti^{4+} pyroxene from the Allende meteorite (from Mao & Bell 1974). (*a*) polarized spectra of the Allende pyroxene at 1 atmosphere; (*b*)—next page—polarized spectra at 1 bar, 20 kbar, and 40 kbar. Note that the doublet at 650 nm splits with increasing pressure, the higher energy peak shifting to higher energy and the lower energy peak remaining stationary with rising pressure. (*c*) spectra of polycrystalline pyroxene at very high pressures. The CF bands shift to higher energy and the CT band gains intensity but remains stationary with increasing pressure.

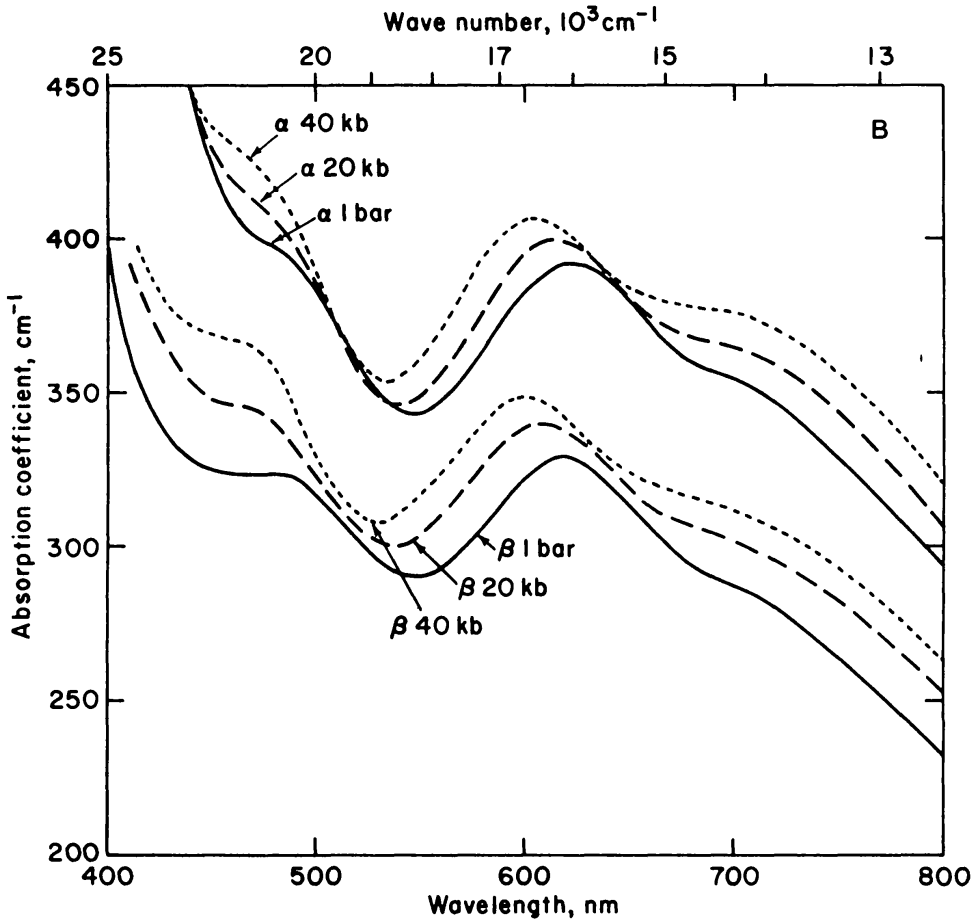

b

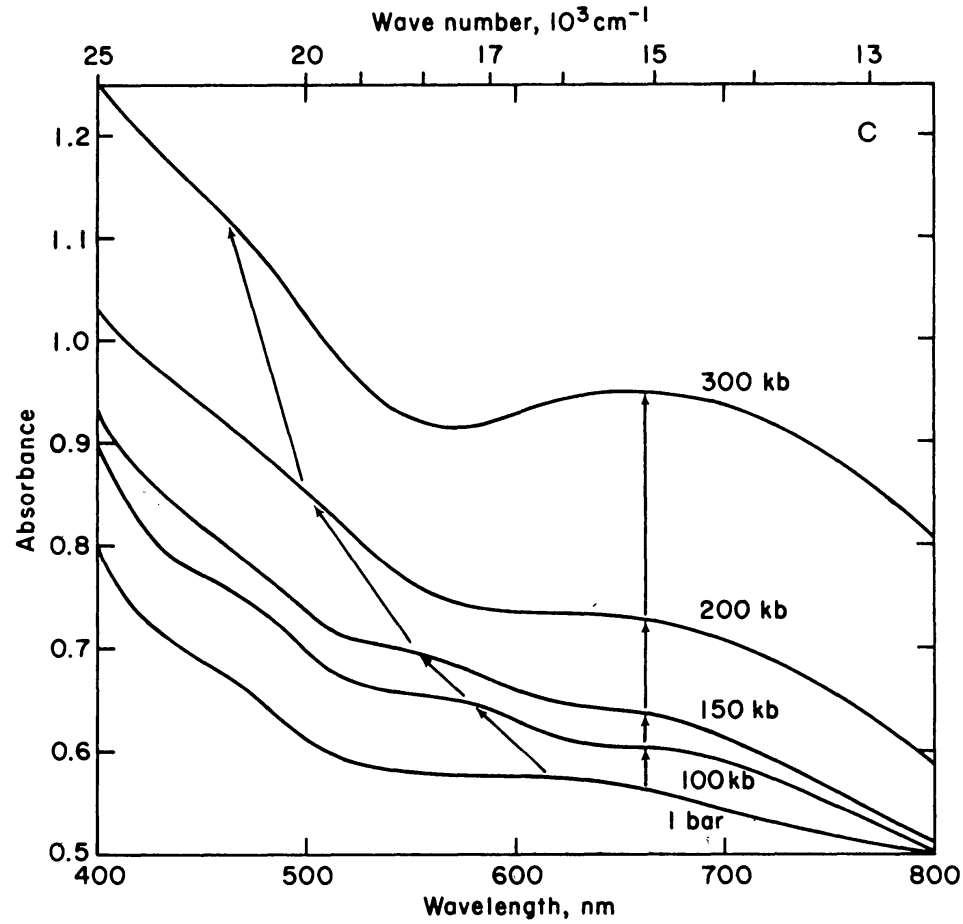

c

Figure 6 (*continued*)

One such pyroxene occurs in the Allende meteorite. Its chemical analysis revealed that it is an iron-free fassaite with coexisting Ti^{3+} and Ti^{4+} ions, having the chemical formula (Dowty & Clark 1973a): $Ca_{1.01}Mg_{0.38}Ti^{3+}_{0.34}Ti^{4+}_{0.14}Al_{0.87}Si_{1.26}O_6$.

The crystal structure of the Allende fassaite, like other calcic clinopyroxenes, contains chains of edge-shared M1 octahedra extending along the *c* axis, and M1-M1 distances are 3.15 Å. Absorption bands in the polarized spectra illustrated in Figure 6 occur around 20,000 cm^{-1} and 16,000 cm^{-1}, and were originally assigned to Ti^{3+} crystal field and $Ti^{3+} \rightarrow Ti^{4+}$ intervalence transitions, respectively (Dowty & Clark 1973a). An alternative assignment, which proposed that both absorption bands originated from crystal field transitions in Ti^{3+} ions in the distorted M1 octahedral sites, was debated (Burns & Huggins 1973, Dowty & Clark 1973b). One method for distinguishing between crystal field and intervalence transitions is to measure pressure-induced variations of the spectra, since increased pressure markedly shifts crystal field bands to higher energies and appreciably intensifies intervalence bands (Abu-Eid 1976, Mao 1976). The conflicting assignments of the Allende pyroxene spectra were subsequently resolved by measurements of the polarized spectra at elevated pressures (Mao & Bell 1974). The spectra illustrated in Figures 6*b* and *c* show that in addition to the bands at 16,000 and 20,000 cm^{-1}, another occurs around 15,000 cm^{-1} and intensifies at high pressures. Furthermore, the position of the 15,000 cm^{-1} band is insensitive to pressure, whereas the 16,000 and 20,000 cm^{-1} bands shift to higher energies with rising pressure, which is consistent with their assignment to Ti^{3+} crystal field transitions. Such pressure measurements demonstrate conclusively that the $Ti^{3+} \rightarrow Ti^{4+}$ intervalence transition in clinopyroxenes occurs at 15,000 cm^{-1}.

$Ti^{3+} \rightarrow Ti^{4+}$ intervalence transitions have been assigned to a number of other natural minerals and synthetic phases (Burns & Vaughan 1975), including andalusite at 20,800 cm^{-1} (Faye & Harris 1969) and tourmaline (Manning 1969). Pressure- and temperature-dependent studies of the absorption spectra of these minerals are required to confirm these assignments.

MINERALS EXHIBITING $Fe^{2+} \rightarrow Ti^{4+}$ INTERACTIONS

The Ti(IV) oxidation state is far more common in terrestrial minerals than Ti(III), and the existence of Fe^{2+}-Ti^{4+} assemblages is potentially very common (Burns & Vaughan 1975). In fact, Fe^{2+}-Fe^{3+} and Fe^{2+}-Ti^{4+} coordination clusters may coexist in the same structure, and give rise to

homonuclear $Fe^{2+} \rightarrow Fe^{3+}$ and heteronuclear $Fe^{2+} \rightarrow Ti^{4+}$ intervalence transitions in the visible region, thereby complicating assignments of absorption bands. As a result some of the bands originally assigned to $Fe^{2+} \rightarrow Fe^{3+}$ intervalence transitions have been reassigned recently to $Fe^{2+} \rightarrow Ti^{4+}$ intervalence transitions. The role of Fe^{2+}-Ti^{4+} clusters in mixed-valence iron minerals is illustrated by the following examples.

Titanian Pyroxenes

One mineral in which Fe^{2+}-Ti^{4+} octahedral clusters occur and Fe^{3+} ions are absent is the pyroxene from the Angra dos Reis meteorite. The composition of the Angra dos Reis fassaite, $Ca_{0.97}Fe_{0.22}Mg_{0.58}Ti_{0.06}Al_{0.43}Si_{1.79}O_6$, together with measurements of its crystal structure and Mössbauer spectrum, indicate that iron and titanium are predominantly in the M1 octahedral sites and that no ferric iron is detectable (Hazen & Finger 1977, Mao et al 1977). Light polarized in the plane of the M1 cations gives rise to a broad intense absorption band centered around 20,600 cm^{-1} (Bell & Mao 1976, Mao et al 1977), which may be assigned to a $Fe^{2+} \rightarrow Ti^{4+}$ intervalence transition. Pressure not only intensifies this band, but also results in a systematic shift of it to *lower* energies, so that at 52 kb it is centered at 19,200 cm^{-1} (Hazen et al 1977). Although such a pressure-induced shift for the $Fe^{2+} \rightarrow Ti^{4+}$ intervalence transition contrasts with the negligible shift observed for the $Ti^{3+} \rightarrow Ti^{4+}$ (Allende pyroxene, Figure 6*c*) and $Fe^{2+} \rightarrow Fe^{3+}$ (vivianite) intervalence transitions, the intensification of the 19,200 cm^{-1} band at elevated pressures is consistent with trends observed for other intervalence transitions.

The $Fe^{2+} \rightarrow Ti^{4+}$ intervalence transition has also been identified in the spectra of titanian pyroxenes from the Moon and in crustal rocks (Burns et al 1976, Dowty 1978). Absorption spectra of terrestrial titanaugites illustrated in Figure 7 are particularly complex. Mössbauer measurements show that Fe^{2+} ions occur in the M1 and M2 sites of the clinopyroxene structure, and also reveal that discrete Fe^{3+} ions occur in both octahedral and tetrahedral coordinations (Burns et al 1976). As a result, polarized absorption spectra of titanaugites contain spin-allowed and spin-forbidden crystal field transitions in multiple-site Fe^{2+} and Fe^{3+} ions in addition to the $Fe^{2+} \rightarrow Fe^{3+}$ and $Fe^{2+} \rightarrow Ti^{4+}$ intervalence transitions (Figure 7). The latter are superimposed on Fe^{3+} crystal field bands which are somewhat intensified due to Fe^{3+} ions in non-centrosymmetric tetrahedral sites.

Alternative assignments of an intervalence transition have been proposed for the spectra of an unusual blue titanian omphacite (Curtis et al 1975). An intense absorption band centered around 15,000 cm^{-1} which shifted to lower energies at 40 kb was originally interpreted as a

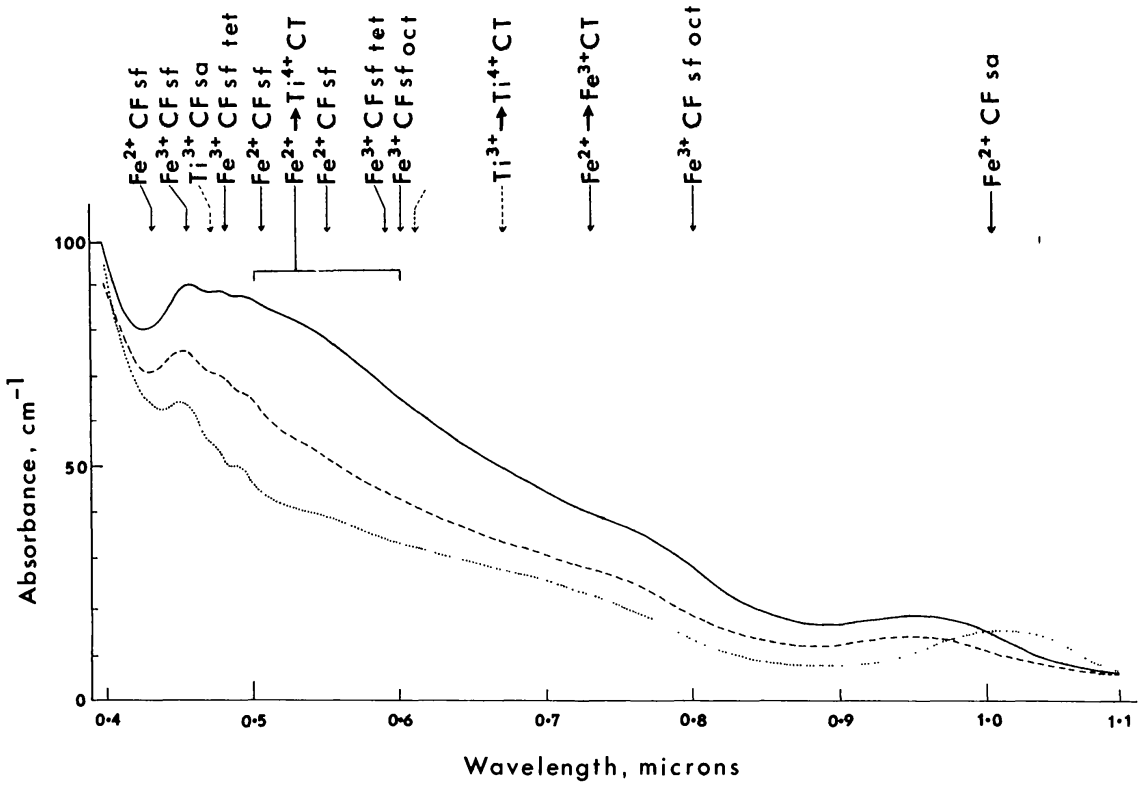

Figure 7 Polarized absorption spectra of a terrestrial titanaugite (from Burns et al 1976). ———, – – – – –, and ····· correspond to Z, Y, and X polarizations, respectively. Assignments of peaks and inflections in the absorption spectra are shown: CF sa: crystal field, spin-allowed; CF sf: crystal field, spin-forbidden; CT: intervalence charge transfer; oct: octahedral; tet: tetrahedral.

$Fe^{2+} \rightarrow Fe^{3+}$ intervalence transition (Abu-Eid 1976). Recently, however, the same band has been assigned to a $Fe^{2+} \rightarrow Ti^{4+}$ transition (Strens et al 1980). The dual assignments remain unresolved at this time.

Kyanite

The major feature in the visible-region spectra of blue kyanites is an intense polarization-dependent band at 16,500 cm^{-1} with a prominent shoulder in the region 11,500–12,500 cm^{-1} (Faye & Nickel 1969a, White & White 1967). The 16,500 cm^{-1} band was assigned to a $Fe^{2+} \rightarrow Fe^{3+}$ intervalence transition (Faye & Nickel 1969a, Faye 1971) between Fe^{2+} and Fe^{3+} ions located in chains of edge-shared $[AlO_6]$ octahedra in the kyanite structure, in which Al-Al distances are 2.76–2.88 Å (Burnham 1963). The shoulder at 12,500 cm^{-1} was attributed to a spin-allowed crystal field transition in octahedral Fe^{2+} ions. Mössbauer spectroscopy subsequently confirmed that octahedral Fe^{2+} and Fe^{3+} ions coexist in blue kyanites (Parkin et al 1977). However, reported correlations of the

intensity of the blue color with Ti contents of kyanites (White & White 1967, Rost & Simon 1972) led to the suggestion that the 16,500 cm^{-1} band is due instead to the $Fe^{2+} \rightarrow Ti^{4+}$ intervalence transition (Smith & Strens 1976). A coupled substitution of Fe^{2+} and Ti^{4+} for two Al^{3+} ions was assumed, since this maintains local charge balance within the structure. It also allows for a high probability of Fe^{2+}-Ti^{4+} couples to exist in adjacent sites, which is necessary to explain the intensity of absorption with rather low concentration of Ti. The shoulder at 11,500–12,500 cm^{-1}, like the 16,500 cm^{-1} band, intensifies at low temperatures, leading the shoulder to be reassigned to a $Fe^{2+} \rightarrow Fe^{3+}$ intervalence transition (Smith & Strens 1976).

Sapphire

A similar assignment to that suggested for the kyanite spectra has been proposed for absorption bands in sapphire (Smith & Strens 1976). The corundum structure consists of hexagonal close-packed oxygen ions in which $[AlO_6]$ octahedra share faces parallel to the *c* axis and share edges perpendicular to *c*. Thus, two types of cation → cation interactions are possible in the corundum structure. Crystal growth studies have established that minor amounts of both Fe and Ti must be added to Al_2O_3 to generate the blue coloration of sapphire. In polarized spectra of synthetic sapphires (Ferguson & Fielding 1972, Eigenmann et al 1972), bands at 17,000 cm^{-1} and 12,900 cm^{-1} occur only when Fe and Ti are both present, while a band at about 11,500 cm^{-1} occurs when Fe alone is present. These bands intensify at low temperatures, indicating that they are intervalence transitions (Smith & Strens 1976, Smith 1978b). A fourth band has been identified at 9,700 cm^{-1} (Lehmann & Harder 1970). It is apparent that Fe-Ti interactions in the corundum structure are important factors determining the color and spectra of sapphire. The following assignments are generally accepted for the intervalence transitions in the sapphire spectra:

17,000 cm^{-1}:	$Fe^{2+} \rightarrow Ti^{4+}$	perpendicular to *c*,
12,900 cm^{-1}:	$Fe^{2+} \rightarrow Ti^{4+}$	parallel to *c*,
11,150 cm^{-1}:	$Fe^{2+} \rightarrow Fe^{3+}$	perpendicular to *c*,
9,700 cm^{-1}:	$Fe^{2+} \rightarrow Fe^{3+}$	parallel to *c*.

Hematite-Ilmenite Solid Solutions

The Fe-Ti octahedral clusters producing the color of sapphire are also responsible for electron delocalization in the hematite-ilmenite solid solution series, $(1\text{-}x)Fe_2O_3.xFeTiO_3$, which is isostructural with corundum. The Fe^{3+} ions in hematite occupy face-shared and edge-shared $[FeO_6]$

octahedra as in corundum, with Fe-Fe distances 2.89 Å and 2.97 Å parallel and perpendicular, respectively, to the c axis (Blake et al 1970). In ilmenite Fe^{2+} and Ti^{4+} ions are ordered so as to be coupled in the face-shared octahedra (Fe-Ti = 2.94 Å), while planes of edge-shared $[FeO_6]$ and $[TiO_6]$ octahedra alternate along the c axis (Fe-Fe = 3.00 Å; Ti-Ti = 2.99 Å) (Raymond & Wenk 1971). A Mössbauer study of the ilmenite-hematite series demonstrated that all Fe^{2+} ions in hematite-rich samples participate in electron delocalization with an equal number of Fe^{3+} ions (Warner et al 1972). Electron delocalization continues for values of x as great as 0.60, but no delocalization is observed in the composition range $0.75 < x < 1.00$. The cations are believed to be completely disordered in the range $0 < x < 0.6$, so that $Fe^{2+} \rightarrow Fe^{3+}$ electron delocalization occurs both between face-shared and edge-shared octahedra. Cation ordering increases in the range $0.60 < x < 0.75$, with the result that $Fe^{2+} \rightarrow Fe^{3+}$ electron delocalization between face-shared octahedra predominates. Between $0.75 < x < 1.00$, Ti effectively blocks electron delocalization between Fe^{2+} and Fe^{3+} ions. Nevertheless, a prominent broad band centered around 16,000 cm^{-1} in the diffuse reflectance spectrum of ilmenite (Adams 1975) has been attributed to a $Fe^{2+} \rightarrow Ti^{4+}$ intervalence transition.

Other Examples

The $Fe^{2+} \rightarrow Ti^{4+}$ intervalence transition is believed to contribute to visible–near ultraviolet spectra of lunar regolith and synthetic Fe-Ti silicate glasses (Adams 1975, Bell et al 1976, Wells & Hapke 1977, Osborne et al 1978, Nolet et al 1979). Other minerals to which $Fe^{2+} \rightarrow Ti^{4+}$ intervalence CT has been assigned (Burns & Vaughan 1975) include andalusite (Faye & Harris 1969, Smith 1977), micas (Faye 1968, Smith 1978b), tourmaline (Manning 1969, Smith 1977, 1978a), and vesuvianite (Manning 1975). They might also occur in neptunite, aenigmatite, and taramellite.

Besides schorlomites (Schwartz et al 1980) and hematite-ilmenite solid-solutions (Warner et al 1972), electron delocalization behavior in Fe-Ti minerals has been observed in magnetite-ulvöspinel solid solutions (Banerjee et al 1967, Jensen & Shive 1973, O'Donovan & O'Reilly 1980). The latter have important implications in geomagnetism.

CONCLUSIONS

Intervalence transitions and electron delocalization phenomena between coexisting cations of Fe and Ti continue to be conspicuous in several rock-forming minerals. In many instances, confusion over previous assignments of visible-region and Mössbauer spectra has been clarified by recent

controlled spectral measurements spanning wider ranges of temperatures, pressures, and mineral specimens. Continued critical measurements are still required for outstanding controversial minerals, and additional examples should be sought of phases exhibiting light-induced electron transfer phenomena between coexisting transition metal ions. Understanding the mechanism of such electronic transitions will broaden the scope of their applications in the earth and planetary sciences beyond explanations of color, pleochroism, and magnetism of minerals; deductions about geomagnetic, geoelectric, and radiative heat transfer properties of the Earth's interior; and interpretations of remote-sensed reflectivity spectral profiles of regoliths on the Moon, Mars, and Mercury.

ACKNOWLEDGMENTS

Many of the results and interpretations of intervalence transitions in minerals have resulted from research by and discussions with Dr. F. E. Huggins, Dr. R. M. Abu-Eid, Dr. C. M. Sung, Dr. K. M. Parkin, Margery Osborne, Kenneth Schwartz, Daniel Nolet, and Catherine McCammon at M.I.T., and with Dr. G. R. Rossman, Dr. D. S. Goldman, Dr. P. M. Bell, Dr. H. K. Mao, Dr. G. Smith, and Dr. G. Amthauer. Mrs. Virginia Mee Burns assisted with bibliographic research. The research is supported by a grant from the National Aeronautics and Space Administration (grant no. NSG-7604).

Literature Cited

Abu-Eid, R. M. 1976. Absorption spectra of transition metal bearing minerals at high pressures. In *The Physics and Chemistry of Minerals and Rocks*, ed. R. G. J. Strens, pp. 641–75. London: Wiley

Abu-Eid, R. M., Langer, K., Seifert, F. 1978. Optical absorption and Mössbauer spectra of purple and green yoderite, a kyanite-related mineral. *Phys. Chem. Miner.* 3:271–89

Adams, J. B. 1975. Uniqueness of visible and near-infrared diffuse reflectance spectra of pyroxenes and other rock-forming minerals. Chapter 1. In *Infrared and Raman Spectroscopy of Lunar and Terrestrial Minerals*, ed. C. Karr, Jr., pp. 1–38. New York: Academic

Aldridge, L. P., Bancroft, G. M., Fleet, M. E., Herzberg, C. T. 1978. Omphacite studies, II. Mössbauer spectra of C2/c and P2/n omphacites. *Am. Mineral.* 63:1107–15

Allen, G. C., Hush, N. S. 1967. Intervalence absorption. Part I. Qualitative evidence for intervalence transfer absorption in inorganic systems in solution and in the solid state. In *Progr. Inorg. Chem.* 8:357–90

Amthauer, G. 1980. ^{57}Fe Mössbauer study of babingtonite. *Am. Mineral.* 65:157–62

Amthauer, G., Annersten, H., Hafner, S. S. 1977. The Mössbauer spectrum of ^{57}Fe in titanium-bearing andradites. *Phys. Chem. Miner.* 1:399–413

Amthauer, G., Langer, K., Schliestedt, M. 1980. Thermally activated electron delocalization in deerite. *Phys. Chem. Miner.* 6:19–30

Annersten, H. 1974. Mössbauer studies of natural biotites. *Am. Mineral.* 59:143–51

Annersten, H., Olesch, M., Seifert, F. A. 1978. Ferric iron in orthopyroxene: a Mössbauer spectroscopic study. *Lithos* 11:301–10

Araki, T., Zoltai, T. 1972. Crystal structure of babingtonite. *Z. Krist.* 135:355–75

Bancroft, G. M. 1979. Mössbauer spectroscopic studies of the chemical state of iron in silicate minerals. *J. Phys.* 40:C2–464–71

Bancroft, G. M., Brown, J. R. 1975. A Mössbauer study of coexisting hornblendes and biotites: quantitative Fe^{3+}/Fe^{2+} ratios. *Am. Mineral.* 60:265–72

Bancroft, G. M., Burns, R. G. 1969. Mössbauer and absorption spectral studies of alkali amphiboles. *Miner. Soc. Am. Spec. Pap.* 2:137–48

Bancroft, G. M., Burns, R. G., Stone, A. J. 1968. Applications of the Mössbauer effect to silicate mineralogy. II. Iron silicates of unknown and complex crystal structures. *Geochim. Cosmochim. Acta* 32:547–59

Bancroft, G. M., Williams, P. G. L., Essene, E. J. 1969. Mössbauer spectra of omphacites. *Miner. Soc. Am. Spec. Pap.* 2:59–65

Banerjee, S. K., O'Reilly, W., Gibb, T. C., Greenwood, N. 1967. The behavior of ferrous ions in iron-titanium spinels. *J. Phys. Chem. Solids* 28:1323–35

Bell, P. M., Mao, H. K. 1976. Crystal-field spectra of fassaite from the Angra dos Reis meteorite. *Ann. Rep. Geophys. Lab. Carnegie Inst. Yearb.* 75:701–5

Bell, P. M., Mao, H. K., Weeks, R. A. 1976. Optical spectra and electron paramagnetic resonance of lunar and synthetic glasses: a study of the effects of controlled atmosphere, composition, and temperature. *Proc. 7th Lunar Sci. Conf., Suppl. 7, Geochim. Cosmochim. Acta* 3:2543–59

Beran, A., Bittner, H. 1974. Untersuchungen zur Kristallchemie des Ilvaits. *Tschermaks Mineral. Petrog. Mitt.* 21:11–29

Blake, R. L., Zoltai, T., Hessevick, R. E., Finger, L. W. 1970. Refinement of hematite crystal structure. *US Bur. Mines Rep. No. 7384*, pp. 1–20

Borg, R. J., Borg, I. Y. 1980. Mössbauer study of behavior of oriented single crystals of riebeckite at low temperatures and their magnetic properties. *Phys. Chem. Miner.* 5:219–34

Brown, D. B., ed. 1980. *Mixed Valence Compounds. Theory and Applications in Chemistry, Physics, Geology, and Biology* Dordrecht: Reidel. 519 pp.

Brown, G. E., Gibbs, G. V. 1969. Refinement of the crystal structure of osumilite. *Am. Mineral.* 54:101–16

Buerger, M. J., Burnham, C. W., Peacor, D. R. 1962. Assessment of several structures proposed for tourmaline. *Acta Crystallog.* 15:583–90

Burnham, C. W. 1963. Refinement of the structure of kyanite. *Z. Kristallogr.* 118:337–60

Burnham, C. W., Ohashi, Y., Hafner, S. S., Virgo, D. 1971. Cation distribution and atomic thermal vibrations in an iron-rich orthopyroxene. *Am. Mineral.* 56:850–76

Burns, R. G. 1970. *Mineralogical Applications of Crystal Field Theory.* Cambridge Univ. Press. 224 pp.

Burns, R. G. 1972. Mixed valencies and site occupancies of iron in silicate minerals from Mössbauer spectroscopy. *Can. J. Spectrogr.* 17:51–59

Burns, R. G. 1976. Partitioning of transition metals in mineral structures of the mantle. In *The Physics and Chemistry of Minerals and Rocks*, ed. R. G. J. Strens, pp. 555–72. London:Wiley

Burns, R. G., Greaves, C. J. 1971. Correlations of infrared and Mössbauer site population measurements of actinolites. *Am. Mineral.* 56:2010–33

Burns, R. G., Huggins, F. E. 1973. Visible absorption spectra of a Ti^{3+} fassaite from the Allende meteorite: A discussion. *Am. Mineral.* 58:955–61

Burns, R. G., Vaughan, D. J. 1975. Polarized electronic spectra. Chapter 2. In *Infrared and Raman Spectroscopy of Lunar and Terrestrial Minerals*, ed. C. Karr, Jr., pp. 39–72. New York:Academic

Burns, R. G., Abu-Eid, R. M., Huggins, R. E. 1972. Crystal field spectra of lunar pyroxenes. *Proc. 3rd Lunar Sci. Conf., Suppl. 3, Geochim. Cosmochim. Acta* 1:533–43

Burns, R. G., Parkin, K. M., Loeffler, B. M., Abu-Eid, R. M., Leung, I. S. 1976. Visible-region spectra of the moon: progress toward characterizing the cations in Fe-Ti bearing minerals. *Proc. 7th Lunar Sci. Conf., Suppl. 7, Geochim. Cosmochim. Acta* 3:2561–78

Burns, R. G., Nolet, D. A., Parkin, K M., McCammon, C. A., Schwartz, K. B. 1980. Mixed-valence minerals of iron and titanium: correlations of structural, Mössbauer, and electronic spectral data. In *Mixed Valence Compounds. Theory and Applications in Chemistry, Physics, Geology, and Biology*, ed. D. B. Brown. Dordrecht: Reidel. 295–336

Cannillo, E., Mazzi, F., Fang, J. H., Robinson, P. D., Ohya, Y. 1971. The crystal structure of aenigmatite. *Am. Mineral.* 56:427–46

Carmichael, I. S. E., Fyfe, W. S., Machin, D. J. 1966. Low spin ferrous iron in the iron silicate deerite. *Nature* 211:1389

Clark, J. R., Appleman, D. E., Papike, J. J. 1969. Crystal-chemical characterization of clinopyroxenes based on eight new structure refinements. *Mineral. Soc. Am. Spec. Pap.* 2:31–50

Cullen, J. R., Callen, E. 1971. Band theory of multiple ordering and the metal-semiconductor transition in magnetite. *Phys. Rev. Lett.* 26:236–38

Curtis, L., Gittins, J., Kocman, V., Rucklidge, J. C., Hawthorne, F. C., Ferguson, R. B. 1975. Two crystal structure refinements of a P2/n titanium ferro-omphacite. *Can. Mineral.* 13:62–67

Day, P. 1976. Mixed valence chemistry and metal chain compounds. In *Low Dimensional Cooperative Phenomena*, ed. H. J. Keller, pp. 191–214. New York Plenum

Dowty, E. 1978. Absorption optics of low symmetry crystals—Application to titanian clinopyroxene spectra. *Phys. Chem. Miner.* 3:173–81

Dowty, E., Clark, J. R. 1973a. Crystal structure refinement and visible-region absorption spectra of a Ti^{3+} fassaite from the Allende meteorite. *Am. Mineral.* 58:230–242

Dowty, E. Clark, J. R. 1973b. Crystal-structture refinement and optical properties of a Ti^{3+} fassaite from the Allende meteorite: Reply. *Am. Mineral.* 58:962–64

Eigenmann, K., Kurtz, K., Gunthard, H. H. 1972. Solid state reactions and defects in doped Verneuil sapphire. *Helv. Phys. Acta* 45:452–80

Ernst, W. G., Wai, C. M. 1970. Mössbauer, infrared, X-ray, and optical study of cation ordering and dehydrogenation in natural and heat treated sodic amphiboles. *Am. Mineral.* 55:1226–58

Evans, B. J., Amthauer, G. 1980. The electronic structure of ilvaite and the pressure and temperature dependence of its ^{57}Fe Mössbauer spectrum. *J. Phys. Chem. Solids.* 41:985–1001

Farrell, E. F., Newnham, R. E. 1967. Electronic and vibrational absorption spectra in cordierite. *Am. Mineral.* 52:380–88

Faye, G. H. 1968. The optical absorption spectra of iron in six-coordinate sites in chlorite, biotite, phlogopite and vivianite. Some aspects of pleochroism in the sheet silicates. *Can. Mineral.* 9:403–25

Faye, G. H. 1971. On the optical spectra of di- and tri- valent iron in corundum: a discussion. *Am. Mineral.* 56:344–50

Faye, G. H. 1972. Relationship between crystal-field splitting parameter, "Δ_{VI}" and M_{host}-O bond distance as an aid in the interpretation of absorption spectra of Fe^{2+}-bearing materials. *Can. Mineral.* 11:473–87

Faye, G. H., Harris, D. C. 1969. On the origin and pleochroism in andalusite from Brazil. *Can. Mineral.* 10:47–56

Faye, G. H., Hogarth, D. D. 1969. On the origin of "reverse pleochrosim" of a phlogopite. *Can. Mineral.* 10:25–34

Faye, G. H., Nickel, E. H. 1969a. On the origin of color and pleochroism of kyanite. *Can. Mineral.* 10:35–46

Faye, G. H., Nickel, E. H. 1969b. The effect of charge transfer processes on the colour and pleochroism of amphiboles. *Can. Mineral.* 10:616–35

Faye, G. H., Manning, P. G., Nickel, E. H. 1968. The polarized optical absorption spectra of tourmaline, cordierite, chloritoid, and vivianite: ferrous-ferric electronic interaction as a source of pleochroism. *Am. Mineral.* 53:1174–1201

Faye, G. H., Manning, P. G., Gosselin, J. R., Tremblay, R. J. 1974. Optical absorption spectra of tourmaline: importance of charge transfer processes. *Can. Mineral.* 12:370–80

Ferguson, J., Fielding, P. E. 1972. The origins of the colours of natural yellow, blue, and green sapphires. *Aust. J. Chem.* 25:1371–85

Fleet, M. E. 1977. The crystal structure of deerite. *Am. Mineral.* 62:990–98

Fleet, S. G., Megaw, H. D. 1962. The crystal structure of yoderite. *Acta Crystallogr.* 15:721–28

Frank, E., Banbury, D. St. P. 1974. A study of deerite by the Mössbauer effect. *J. Inorg. Nucl. Chem.* 36:1725–30

Gérard, A., Grandjean, F. 1971. Observations by the Mössbauer effect of an electron hopping process in ilvaite. *Solid State Comm.* 9:1845–49

Gibbs, G. V. 1966. The polymorphism of cordierite. I. The crystal structure of low cordierite. *Am. Mineral.* 51:1068–87

Gibbs, G. V., Breck, D. W., Meagher, E. P. 1968. Structural refinements of hydrous and anhydrous synthetic beryl, $Al_2(Be_3Si_6)O_{18}$ and emerald $Al_{1.9}Cr_{0.1}(Be_3Si_6)O_{18}$. *Lithos* 1:275–85

Goldman, D. S. 1979. A re-evaluation of the Mössbauer spectroscopy of calcic amphiboles. *Am. Mineral.* 64:109–18

Goldman, D. S., Rossman, G. R. 1977a. The spectra of iron in orthopyroxene revisited: the splitting of the ground state. *Am. Mineral.* 62:151–57

Goldman, D. S., Rossman, G. R. 1977b. The identification of Fe^{2+} in the M(4) site of calcic amphiboles. *Am. Mineral.* 62:205–16

Goldman, D. S., Rossman, G. R. 1978. The site distribution of iron and anomalous biaxiality in osumilite. *Am. Mineral.* 63:490–98

Goldman, D. S., Rossman, G. R., Dollase, W. A. 1977. Channel constituents in cordierite. *Am. Mineral.* 62:1144–57

Goldman, D. S., Rossman, G. R., Parkin, K. M. 1978. Channel constituents in beryl. *Phys. Chem. Miner.* 3:225–35

Grandjean, F., Gérard, A. 1975. Analysis by Mössbauer spectroscopy of the electron

hopping process in ilvaite. *Solid State Comm.* 16:553–56
Haga, N., Takéuchi, Y. 1976. Neutron diffraction study of ilvaite. *Z. Kristallogr.* 144:161–74
Hamilton, W. C. 1958. Neutron diffraction study of the 119K transition in magnetite. *Phys. Rev.* 110:1050–57
Hawthorne, F. C. 1976. The crystal chemistry of the amphiboles. V. The structure and chemistry of arfvedsonite. *Can. Mineral.* 14:346–56
Hazen, R. M., Burnham, C. W. 1973. The crystal structures of one-layer phlogopite and annite. *Am. Mineral.* 58:889–900
Hazen, R. M., Finger, L. W. 1977. Crystal structure and compositional variation of Angra dos Reis fassaite. *Earth Planet. Sci. Lett.* 35:357–62
Hazen, R. M., Bell, P. M., Mao, H. K. 1977. Polarized absorption spectra of Angra dos Reis fassaite to 52 k bar. *Ann. Rep. Geophys. Lab., Carnegie Inst. Washington Yearb.* 76:515–16
Heilmann, I. U., Olsen, N. B., Olsen, J. S. 1977. Electron hopping and temperature dependent oxidation states of iron in ilvaite studied by Mössbauer effect. *Phys. Scr.* 15:285–88
Hermon, E., Simkin, D. J., Donnay, G., Muir, W. B. 1973. The distribution of Fe^{2+} and Fe^{3+} in iron-bearing tourmalines: a Mössbauer study. *Tschermaks Mineral. Petrogr. Mitt.* 19:124–32
Higgins, J. B., Ribbe, P. H. 1979. Sapphirine II. A neutron and x-ray diffraction study of $(Mg\text{-}Al)^{VI}$ and $(Si\text{-}Al)^{VI}$ ordering in monoclinic sapphirine. *Contrib. Mineral. Petrol.* 68:357–68
Higgins, J. B., Ribbe, P. H., Herd, R. K. 1979. Sapphirine I. Crystal chemical contributions. *Contrib. Mineral. Petrol.* 68:349–56
Huggins, F. E., Virgo, D. Huckenholz, H. G. 1977a. Titanium-containing silicate garnets. I. The distribution of Al, Fe^{3+} and Ti^{4+} between octahedral and tetrahedral sites. *Am. Mineral.* 62:475–90
Huggins, F. E., Virgo, D., Huckenholz, H. G. 1977b. Titanium-containing silicate garnets. II. The crystal chemistry of melanites and schorlomites. *Am. Mineral.* 62:646–65
Hush, N. S. 1967. Intervalence-transfer absorption. Part 2. Theoretical considerations and spectroscopic data. *Progr. Inorg. Chem.* 8:391–444
Jensen, S. D., Shive, P. N. 1973. Cation distribution in sintered titano-magnetites. *J. Geophys. Res.* 78:8474–80
Kosoi, A. L. 1976. The structure of babingtonite. *Sov. Phys. Crystallogr.* 20:446–51
Kundig, W., Hargrove, R. S. 1969. Electron hopping in magnetite. *Solid State Comm.* 7:223–27
Lehmann, G., Harder, H. 1970. Optical spectra of di- and trivalent iron in corundum. *Am. Mineral.* 55:98–105 (See also: *Am. Mineral.* 56:349–50)
Littler, J. G. F., Williams, R. J. P. 1965. Electrical and optical properties of crocidolite and some other iron compounds. *J. Chem. Soc.*, pp. 6368–71
Loeffler, B. M., Burns, R. G. 1976. Shedding light on the color of gems and minerals. *Am. Sci.* 64:636–47
Loeffler, B. M., Burns, R. G., Tossell, J. A., Vaughan, D. J., Johnson, K. H. 1974. Charge transfer in lunar materials: interpretation of ultra-violet-visible spectral properties of the moon. *Proc. 5th Lunar Sci. Conf., Suppl. 5, Geochim. Cosmochim. Acta* 3:3007–16
Loeffler, B. M., Burns, R. G., Tossell, J. A. 1975. Metal-metal charge transfer transitions: interpretations of visible-region spectra of the moon and lunar materials. *Proc. 6th Lunar Sci. Conf., Suppl. 6, Geochim. Cosmochim. Acta* 3:2663–76
Lotgering, F. K., van Diepen, A. M. 1977. Electron exchange between Fe^{2+} and Fe^{3+} ions on octahedral sites in spinels studied by means of paramagnetic Mössbauer spectra and suceptibility measurements. *J. Phys. Chem. Solids* 38:565–72
MacCarthy, G. R. 1926. Colors produced by iron in minerals and the sediments. *Am. J. Sci.* 12:16–36
Manning, P. G. 1969. An optical absorption study of the origin of colour and pleochroism in pink and brown tourmalines. *Can. Mineral.* 9:678–90
Manning, P. G. 1975. Charge-transfer processes and the origin of colour and pleochroism of some titanium-rich vesuvianites. *Can. Mineral.* 13:110–16
Manning, P. G., Harris, D. C. 1970. Optical-absorption and electron microprobe studies of some high-Ti andradites. *Can. Mineral.* 10:260–71
Manning, P. G., Nickel, E. H. 1969. A spectral study of the origin of colour and pleochroism of a titanaugite from Kaiserstuhl and of a riebeckite from St. Peter's Dome, Colorado, *Can. Mineral.* 10:71–83
Mao, H. K. 1976. Charge-transfer processes at high pressure. In *The Physics and Chemistry of Minerals and Rocks*, ed. R. G. J. Strens, pp. 573–81
Mao, H. K., Bell, P. M. 1974. Crystal-field effects of trivalent titanium in fassaite from the Pueblo de Allende meteorite. *Ann. Rep. Geophys. Lab., Carnegie Inst. Washington Yearb.* 73:488–92

Mao, H. K., Bell, P. M., Virgo, D. 1977. Crystal-field spectra of fassaite from the the Angra dos Reis meteorite. *Earth Planet. Sci. Lett.* 35:352–56

Martinet, J., Martinet, A. 1952. Pleochroism and structure of natural silicates. *Bull. Soc. Chem. France* 19:563–65

McCammon, C. A., Burns, R. G. 1980. The oxidation mechanism of viviante as studied by Mössbauer spectroscopy. *Am. Mineral.* 65:361–66

Merlino, S. 1980. Crystal structure of sapphirine-lTc *Z. Kristallogr.* 151:91–100

Mitchell, J. T., Bloss, F. D., Gibbs, G. V. 1971. Examination of the actinolite structure and four other C2/m amphiboles in terms of double bonding. *Z. Kristallogr.* 133:273–300

Moore, P. B. 1969. The crystal structure of sapphirine. *Am. Mineral.* 54:31–49

Moore, R. K., White, W. B. 1971. Intervalence electron transfer effects in the spectra of the melanite garnets. *Am. Mineral.* 56:826–40

Mori, H., Ito, T. 1950. The structure of vivianite and symplesite. *Acta Crystallogr.* 3:1–6

Newnham, R. E., de Haan, Y. E. 1962. Refinement of the α-Al_2O_3, Ti_2O_3, V_2O_3, and Cr_2O_3 structures. *Z. Kristallogr.* 117:235–37

Nolet, D. A. 1978. Electron delocalization observed in the Mössbauer spectrum of ilvaite. *Solid State Comm.* 20:719–22

Nolet, D. A., Burns, R. G. 1978. Temperature dependent Fe^{2+}-Fe^{3+} electron delocalization in ilvaite. *Geophys. Res. Lett.* 4:821–24

Nolet, D. A., Burns, R. G. 1979. Ilvaite: a study of temperature dependent electron delocalization by the Mössbauer effect. *Phys. Chem. Miner.* 4:221–34

Nolet, D. A., Burns, R. G., Flamm, S. L., Besancon, J. R. 1979. Spectra of Fe-Ti silicate glasses: implications to remote-sensing of planetary surfaces. *Proc. Lunar Planet. Sci. Conf., 10th, Suppl. II, Geochim. Cosmochim. Acta* 2:1775–86

Novak, G. A., Gibbs, G. V. 1971. The crystal chemistry of the silicate garnets. *Am. Mineral.* 56:791–825

O'Donovan, J. B., O'Reilly, W. 1980. The temperature dependent cation distribution in titanomagnetites. *Phys. Chem. Miner.* 6:235–43

Osborne, M. D., Parkin, K. M., Burns, R. G. 1978. Temperature-dependence of Fe-Ti spectra in the visible region: implications to mapping Ti concentrations of hot planetary surfaces. *Proc. Lunar Planet. Sci. Conf., 9th, Suppl. 9, Geochim. Cosmochim. Acta* 3:2949–60

Papike, J. J., Clark, J. 1968. The crystal structure and cation distribution of glaucophane. *Am. Mineral.* 53:1156–73

Paques-Ledent, M. T., Grandjean, F., Gerard, A. 1977. Chemical formula of ilvaite: infrared and Mössbauer data. *Bull. Soc. R. Sci. Liege* 46:337–42

Parkin, K. M., Loeffler, B. M., Burns, R. G. 1977. Mössbauer spectra of kyanite, aquamarine, and cordierite showing intervalence charge transfer. *Phys. Chem. Miner.* 1:301–11

Pollak, H. 1976. Charge transfer in cordierite. *Phys. Stat. Sol.* 74:K31–K34

Pollak, H., Quartier, R., Bruyneel, W., Walter, P. 1979. Electron relaxation in deerite. *J. Phys.* 40:C2–455

Raymond, K. N., Wenk, H. R. 1971. Lunar ilmenite (refinement of the crystal structure). *Contrib. Mineral. Petrol.* 30:135–40

Robbins, D. W., Strens, R. G. J. 1972. Charge transfer in ferromagnesian silicates: the polarized electronic spectra of trioctahedral micas. *Mineral. Mag.* 38:551–63

Robin, M. B., Day, P. 1967. Mixed valence chemistry–a survey and classification. *Adv. Inorg. Chem. Radiochem.* 10:247–423

Rost, F., Simon, E. 1972. Zur Geochemie und Färbung des Cyanits. *Neues Jahrb. Mineral. Monatsh.* 9:383–95

Sawatzky, G. A., Coey, J. M. D., Morrish, A. H. 1969. Mössbauer study of electron hopping in the octahedral sites of Fe_3O_4. *J. Appl. Phys.* 40:1402–3

Schwartz, K. B., Nolet, D. A., Burns, R. G. 1980. Mössbauer spectroscopy and crystal chemistry of natural Fe-Ti garnets. *Am. Mineral.* 65:142–53

Smith, G. 1977. Low temperature optical studies of metal-metal charge-transfer transitions in various minerals. *Can. Mineral.* 15:500–7

Smith, G. 1978a. A reassessment of the role of iron in the 5000–30000 cm^{-1} range of the electronic absorption spectra of tourmaline. *Phys. Chem. Miner.* 3:343–73

Smith, G. 1978b. Evidence for absorption by exchange-coupled Fe^{2+}-Fe^{3+} pairs in the near infrared spectra of minerals. *Phys. Chem. Miner.* 3:375–83

Smith, G., Strens, R. G. J. 1976. Intervalence transfer absorption in some silicate, oxide and phosphate minerals. In *The Physics and Chemistry of Minerals and Rocks*, ed. R. G. J. Strens, pp. 583–612. New York: Wiley

Strens, R. G. J., Mao, H. K., Bell, P. M. 1980. Quantitative spectra and optics of some meteoritic and terrestrial titanian

clinopyroxenes. *Phys. Chem. Miner. In* press

Sung, C-M., Abu-Eid, R. M., Burns, R. G. 1974. Ti^{3+}/Ti^{4+} ratios in lunar pyroxenes: implications to depth of origin of mare basalt magma. *Proc. 5th Lunar Sci. Conf., Suppl. 5, Geochim. Cosmochim. Acta* 1:717–26

Townsend, M. G. 1968. Visible charge transfer band in blue sapphire. *Solid State Comm.* 6:81–83

Townsend, M. G. 1970. On the dichroism of tourmaline. *J. Phys. Chem. Solids* 31:2481–88

Verble, J. L. 1974. Temperature-dependent light scattering studies of the Verwey transition and electronic disorder in magnetite. *Phys. Rev. B* 9:5236–48

Verwey, E. J., Haayman, P. W. 1941. Electronic conductivity and transition point of magnetite (Fe_3O_4). *Physica* 8:979–87

Warner, B. N., Shive, P. N., Allen, J. L., Terry, C. 1972. A study of the hematite-ilmenite series by the Mössbauer effect. *J. Geomag. Geoelectr.* 24:353–67

Watson, T. L. 1918. The color change in vivianite and its effect on the optical properties. *Am. Mineral.* 3:159–61

Wells, E., Hapke, B. 1977. Lunar soil: iron and titanium bands in the glass fraction. *Science* 195:977–79

Wenk, H. R. 1974. Howieite, a new type of chain silicate. *Am. Mineral.* 59:86–97

Weyl, W. A. 1951. Light absorption as a result of the interaction of two states of valency of the same element. *J. Phys. Colloid Chem.* 55:507–12

White, E. W., White, W. B. 1967. Electron microprobe and optical absorption study of colored kyanites. *Science* 158:915–17

Wilkins, R. W. T., Farrell, E. F., Naimen, C. S. 1969. The crystal field spectra and dichroism, of tourmaline. *J. Phys. Chem. Solids* 30:43–56

Wood, D. L., Nassau, K. 1968. The characterization of beryl and emerald by visible infrared absorption spectroscopy. *Am. Mineral.* 53:777–800

Yamanaka, T., Takéuchi, Y. 1979. Mössbauer spectra and magnetic features of ilvaites. *Phys. Chem. Miner.* 4:149–59